



Please cite the Published Version

Okafor, KC , Adebisi, B , Akande, AO and Anoh, K (2024) Agile gravitational search algorithm for cyber-physical path-loss modelling in 5G connected autonomous vehicular network. Vehicular Communications, 45. 100685 ISSN 2214-2096

DOI: <https://doi.org/10.1016/j.vehcom.2023.100685>

Publisher: Elsevier

Version: Published Version

Downloaded from: <https://e-space.mmu.ac.uk/634605/>

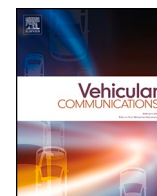
Usage rights:  [Creative Commons: Attribution 4.0](https://creativecommons.org/licenses/by/4.0/)

Additional Information: This is an open access article published in Vehicular Communications, by Elsevier.

Data Access Statement: Data will be made available on request.

Enquiries:

If you have questions about this document, contact openresearch@mmu.ac.uk. Please include the URL of the record in e-space. If you believe that your, or a third party's rights have been compromised through this document please see our Take Down policy (available from <https://www.mmu.ac.uk/library/using-the-library/policies-and-guidelines>)



Agile gravitational search algorithm for cyber-physical path-loss modelling in 5G connected autonomous vehicular network

Kennedy Chinedu Okafor^{a,b,*}, Bamidele Adebisi^b, Akinyinka Olukunle Akande^c, Kelvin Anoh^d

^a Department of Mechatronics Engineering, Federal University of Technology, Owerri, Nigeria

^b School of Engineering, Manchester Metropolitan University, Manchester M1 5GD, UK

^c Department of Electrical and Electronics Engineering, Federal University of Technology, Owerri, Nigeria

^d Department Electrical and Electronic Engineering, University of Chichester, Bognor Regis, UK

ARTICLE INFO

Keywords:

5G
Beyond 5G
6G
Cyber-physical systems
Connected autonomous vehicles
Path loss
Service provisioning

ABSTRACT

Based on the characteristics of the 5 G standard defined in Release 17 by 3GPP and that of the emerging Beyond 5 G (or the so-called 6 G) network, cyber-physical systems (CPSs) used in smart transport network infrastructures, such as connected autonomous vehicles (CAV), will significantly depend on the cellular networks. The 5 G and Beyond 5 G (or 6 G) will operate over millimetre-wave (mmWave) bands. These network standards require suitable path loss (PL) models to guarantee effective communication over the network standards of CAV. The existing PL models suffer heavy signal losses and interferences at mmWave bands and may not be suitable for cyber-physical (CP) signal propagation. This paper develops an Agile Gravitational Search Algorithm (AGSA) that mitigates the PL and signal interference problems in the 5G–NR network for CAV. On top of that, a modified Okumura-Hata model (OHM) suitable for deployment in CP terrestrial mobile networks is derived for the CAV-CPS application. These models are tested on the real-world 5 G infrastructure. Results from the simulated models are compared with measured data for the modified, enhanced model and four other existing models. The comparative evaluation shows that the modified OHM and AGSA performed better than existing OHM, COST, and ECC-33 models by 90%. Also, the modified OHM demonstrated reduced signal interference compared to the existing models. In terms of optimisation validation, the AGSA scheme outperforms the Genetic algorithm, Particle Swarm Optimisation, and OHM models by at least 57.43%. On top of that, the enhanced AGSA outperformed existing PL (i.e., Okumura, Egli, Ericson 999, and ECC-33 models) by at least 67%, thus presenting the potential for efficient service provisioning in 5G-NR driverless car applications.

1. Introduction

Intelligent transport systems (ITS) are now increasingly explored in recent times due to the availability of Sub-6 GHz and millimetre wave (mmWave) agile optimisation techniques for path loss (PL). For example, a UK tech company Oxbotica has recently tested their first autonomous fleet on British streets in London [1]. In addition, the £13.6 million investment in driverless automobiles, which the UK government partially supports, is another step towards showing how autonomous vehicles may function in large European cities [1]. Such evidence shows that the ITS as a part of Cyber-Physical Systems (CPS) can be fully powered by 5/6 G networks [2]. In these systems, an electromagnetic wave's power density fluctuates along its course as it travels across space due to signal attenuation and PL [3]. Therefore, in the research and

design of a CPS link budget, PL models play a significant role, for example, in connected and automated vehicular technologies [4,5]. The reason is that the design of cellular networks requires propagation PL models which are crucial for defining major system characteristics including transmission power, frequency, antenna heights, and so forth.

Several PL models are developed for different propagation environments, such as (indoor, outdoor, urban, suburban, and rural). For instance, alpha-beta-gamma (ABG) and the close-in (CI) free-space schemes have been proposed for 5 G network design in urban micro and macro-cellular situations [6]. In [7], the authors highlighted a signal-denoising network as a localisation strategy for non-line-of-sight (NLOS) propagation in complicated indoor situations. Such signal interference and attenuation along the propagation path lead to PL concerns [8]. This has a significant effect on CPS-CAVs. For instance, most self-driving automobiles are now hindered by inclement weather.

* Corresponding author.

E-mail address: k.okafor@mmu.ac.uk (K.C. Okafor).

<https://doi.org/10.1016/j.vehcom.2023.100685>

Received 23 March 2023; Received in revised form 19 September 2023; Accepted 17 October 2023

Available online 22 October 2023

2214-2096/© 2023 School of Engineering, Manchester Metropolitan University, Manchester M1 5GD, UK. Published by Elsevier Inc. This is an open access article under the CC BY license (<http://creativecommons.org/licenses/by/4.0/>).

Nomenclature

AGSA	Agile Gravitational Search Algorithm	GPS	Global positioning system
ABG	Alpha-beta-gamma	GUI	Graphics user interface
ARQ	Automatic repeat request	HARQ	Hybrid Automatic Repeat reQuest
BPSA	Binary particle swarm algorithm	HPDT	Highly provisioned drive Test
BGP	Binary gravity algorithm	ITS	Intelligent transport systems
BS	Base Station	LOS	line of sight
CAV	Connected Autonomous Vehicles	LTE	Long term Evolution
CPS	Cyber-Physical Systems	MAPE	Mean Absolute Percentage Error
CI	Close-in	MIMO	Multiple-Input, Multiple-Output
5G CP-PL	Cyber-Physical Path loss	OHM	Modified Okumura-Hata model
CP-AGSA	Cyber-physical gravitation search algorithm	mmWave	Millimetre-wave
CPRA	Cyber-Physical regression analysis	MAPE	Mean Absolute Percentage Error
CHMCPSs	Cooperative-heterogeneous mobile wireless CPSs	NIA	Nature-inspired algorithm
CP-AGSA	Cyber-Physical Gravitational Search Algorithm	NLOSLB	Non-LOS link budgets
CLO	Clouded leopard optimisation	GA	Optimised Genetic Algorithm
DL	Deep learning	PL	Path Loss
EISPA	Efficient edge-intelligent service placement algorithm	PSO	Particle Swarm Optimisation
ECCM	Electronic Communication Committee Model	PDMDD	Particle distance, mutual distribution dispersion
FEC	Forward error correction	RANs	Radio access networks
GSA	Gravitational Search Algorithm	RMSE	Root Mean Square Error
GOA	Global optimisation algorithms	STNI	Smart transport network infrastructures
GA	Genetic Algorithms	SOM	Self-organising map
		CUE	5G CAV equipment

Their sensors are hampered by heavy rain, obstructive massive objects, and even snow on the ground making it challenging for cars to discern lane markings. The functions of cameras and lidar on self-driving cars may be significantly reduced in bad weather. Ground-penetrating radar has been proposed by MIT researchers [9]. Self-driving cars use cameras and lidar to navigate, along with extremely detailed maps. The issue is that as visibility declines in weather like rain, snow, fog, and others, so does the use of those devices.

Path loss mitigation in 5 G/6 G RAN and core networks will further deliver ultra-low latency, high bandwidth, flexibility, and smart service provisioning required in CPS deployment use cases. The work [10] achieved novel application service interaction in the 5 G network but suffered greater signal deviation in the channel due to PL. For precise link budget calculations and robust system design, optimal PL modelling is crucial. As noted in [11], poor optimisation with capacity discrepancies resulted from using several appropriate models in current 5 G mmWave propagation within indoor environments. Optimisation efforts in [12] and [13] pointed out that the search space for optimisation (i.e., high dimensional search space) grows exponentially with the size of the PL problem. This makes it impossible to solve these problems using standard optimisation algorithms.

Finding a set of inputs to an objective function that yields a maximum or minimal function evaluation is desirable. Within the 5G-NR CPS, the use of global optimisation algorithms (GOA) to locate the global minima or maxima of the PL function on a given set has not been explored. Employing the Gravitational Search Algorithm (GSA) as a nature-inspired algorithm (NIA) is therefore significant since it explores the gravitational laws as well as laws of motion. While modern deterministic algorithms cannot deliver complex solutions, these optimisation issues are solved using NIA, which has shown considerable success over the past 20 years, particularly when applied to nonlinear real-world optimisation problems [12,13].

A major reason for global optimisation in CPS is that the 5 G CAV deployment enables the multiplexing of virtualised and independent resources on the same physical infrastructure as seen in vehicular-assisted CPSs [14]. Considering a typical smart city application, the CPS offers real-time and gives quality performance within safety-driven transport applications. This is useful in cooperative-heterogeneous

mobile wireless CPSs (CHMCPSs). When applied in transport networks, PL affects the control and coordination of associated aerial-ground mobile systems as a CPS. Typical of this scenario is in the decentralised vehicular dynamics model where mobile swarm-routers are clustered in a communication domain [14]. An obvious intervention is to leverage routing optimisation to transmit signals seamlessly using vehicular drive tests. As a meta-heuristic intelligent optimisation scheme, the advantages of GSA include structural simplicity, fewer parameters, and excellent global optimisation capabilities, algorithm accuracy, amongst others. The GSA method is better than other algorithms [12]. The existing GSA still has issues such as premature convergence, limited local search ability, and a lack of efficient acceleration mechanisms, even though GSA has several advantages over other intelligent calculation approaches.

However, replacing existing PL empirical models with a global optimisation model is crucial. This is a valuable strategy for the current CPS network design and deployment. Most work on 5 G driverless cars and other CPS have not practically explored GSA in context. As a result of the terrain and transmission frequency, existing models cannot predict attenuation and signal interference in 5 G and 4 G LTE-A CPS. This may not be suitable for emerging standards, such as the 6 G. There is a need to highlight and address PL mitigation in CPS, especially in the context of CAV and 5 G networks. The existing global optimisation algorithms lack optimal exploration, and there is a lack of detailed modelling of PL sensitivity based on GSA.

In addition, access control and security aspects for 5 G CAV networks are critical [15,16]. Interesting evidence has shown that the security of channels, applications, and data usage control in 5 G CAV networks must be considered in threat defence-in-depth approaches [17,18]. However, this work focuses on PL modelling considering more precise parameters, regional topology, antenna heights, and other link budget factors that would facilitate attainable CAV 5 G radio coverage.

This paper, therefore, develops an enhanced Agile GSA that can mitigate the effect of PL and signal interference in CP 5 G new radio networks. A typical use case is presented in Wales and can be adapted to high-density traffic environments such as Manchester, London, etc. Finally, an improved cyber-physical PL AGSA has been developed for 5 G radio network service at Sub-6 GHz spectrum frequency.

1.1. Main contributions

The main contributions of this paper are:

- CP-AGSA optimisation method proposed for legacy PL models in CAVs. The optimisation approach addresses PL problems in CPS and works well within 5 G and edge-Fog computing networks.
- Node-Link problem is formulated as a control problem using the proposed CP-AGSA. We incorporated input-to-state traffic parameters and control strategies for effective path planning.
- empirical modelling and analysis of PL prediction using regression analysis. The proposed scheme improves PL estimation accuracy, leading to better signal strength prediction models for CAVs.
- parameter settings and their performance in optimising PL are discussed. Comparative scenarios are used to demonstrate the algorithm's superiority over other optimisation methods in terms of optimized PL values and convergence speed.
- global optimisation performance validation of the CP-AGSA algorithm with existing models in terms of predictive accuracy. Performance metrics such as MAPE and RMSE are used to validate the effectiveness of CP-AGSA.

The remaining parts of this paper are organised into sections. A review of the related works is introduced in [Section 2](#). In [Section 3](#), an existing empirical model is presented. [Section 4](#) discussed the proposed CP-AGSA. In [Section 5](#), a use case scenario was described alongside the data collection methods. [Section 6](#) presented a regression analysis of the path loss models. In [Section 7](#), the Cyber-Physical propagation model validation is discussed. [Section 8](#) presented the result discussions. The global optimisation performance validation was presented in [Section 9](#). [Section 10](#) detailed the noise interference wider implications for this work. [Section 11](#) concludes the paper with specific future directions.

2. Related work

In this section, detailed leading efforts on global optimisation will be discussed while pointing out the limitations. The authors [[13,19](#)] provided discussions on NIA including its application contexts in optimisation problems without considering 5 G CAVs. For instance, the paper [[20](#)] proposed clouded leopard optimisation (CLO) as a new meta-heuristic algorithm inspired by nature with two exploration and exploitation phases. A similar NIA was studied in energy harvester networks [[21](#)] but offered no insight into 5 G PL incidents. Baseline efforts on GSA were studied in [[21,22](#)] though the works lack discussions on PL modelling. In [[23](#)], the authors presented an efficient edge-intelligent service placement algorithm (EISPA). This turns the

service placement problem into finding a globally optimal solution through particle swarm optimisation (PSO). The paper [[24](#)] used unsupervised self-organising map (SOM) learning to provide an intelligent approach for coverage planning as well as a performance optimisation. In terms of evolutionary algorithms/genetic algorithms, significant efforts have been made to date. A good example is discussed in [[25](#)] where the authors focused deeply on problems with constrained optimal characteristics using GA. The limitation is the absence of CP PL exploration. In [[26](#)], the authors explored searched-based differential evolution maps without emphasis on PL mitigations. The authors [[27](#)], applied Swarm-based optimisation algorithms to elastic collision, especially for coding optimisation without any reference to CP PL mitigation. In [[28](#)], ant colony optimisation was applied in identifying the shortest path problem space without PL considerations. The authors [[29](#)] proposed memetic algorithms in vehicular networks, especially for task offloading but failed to look at PL optimisation benefits in their models. In [[30](#)], an artificial bee colony was applied in a multi-strategy construct for path location with no emphasis on 5 G CP-PL intervention. In [[31](#)], the PSO-GSA hybrid was explored in a power despatch challenge. However, the algorithm was not adapted to CP-PL models. The authors [[32](#)] focused on graduated optimisation for optical flow prediction leveraging global matching design. This optimisation algorithm also failed to capture PL improvement within the 5 G CP context.

Authors [[33,34](#)] however pointed out the benefits of GSA such as low solution precision, trapping in local optima, and low convergence rates. For instance, the paper [[35](#)] explored binary GSA to fuse advanced convergent schemes such as the binary particle swarm algorithm (BPSA), binary gravity algorithm (BGP), particle distance, mutual distribution dispersion (PDMDD), and chaotic mutation (CM). These were used to improve convergence performance without considering the computational complexity of PL scenarios.

In non-NIA, extensive research has been conducted to optimise existing 5 G networks in major metropolitan areas [[36,37](#)]. Notably, the prevailing PL prediction models employed for network analysis encompass standards such as COST-231, Egli, Okumura-Hata, Ecc-33, and Ericsson models [[38](#)]. However, many of these conventional PL models exhibit sluggish responsiveness when confronted with diverse terrains and are ill-suited for the demands of 5 G New Radio (NR) networks deployed for autonomous vehicles [[39](#)]. Their inefficiency becomes particularly evident when attempting precise PL analysis in urban settings, largely due to PL variations and signal interference challenges [[40](#)].

A summary of most related works has been highlighted in [Table 1](#). It equally shows that the global optimisation algorithms with various gaps in PL improvements and speed convergence in CAV and other CPS applications.

Table 1
Summary of related works.

Author (Year)	Focus and Coverage	Research Gap	Remarks
Lee et al., (2021) [41]	overlapping multi-state PL model selection for indoor RSS. The GA is applied to reduce the complexity so that the proposed method can be executed in real-time.	PL mitigation strategy suffers from outdoor channel error (severe channel blockage) in 5 G mm-wave.	A more compact PL algorithm is necessary to achieve better performance and compensate for signal loss in CAV full duplex transactions.
Khalid et al., (2020) [42]	Evolutionary algorithm (EA) based methods, such as Artificial Bee Colony (BEE) and PSO algorithms for a hybrid pre-coding system	Interference cancellation, signal blockage, and PL issues were not considered.	An agile model with 5 G network parameters is needed for performance upscaling.
Santana et al., (2022) [43]	Infusion of PL machine Learning optimisation with Bagging and Genetic Algorithms (GA)	PL optimisation in 5 G and beyond encountered a massive surge in network traffic due to more service load demands.	Signal optimisation with an improved PL model is needed to mitigate signal interference.
Chiroma et al., (2023) [44]	ML and DL algorithms to predict PL in wireless systems.	Non-compensation for signal interference, attenuation, path loss, delay, and multipath effect.	An agile cyber-physical PL model is needed to achieve resource optimisation
Mittal et al., (2021) [45]	Comparative analysis amongst ten GSA variants with parameters optimisation.	Poor network connections were identified due to delay and blockage in the channel. The variant of the GSA was not deployed to solve the PL problem in the 5 G NR network. The effect of PLs and interference was not considered	A new CP PL model is necessary to achieve better performance.

2.1. Research gaps

From the existing global optimisation algorithms, PL mitigation in CPS such as CAV in transport systems is yet to be fully addressed. There is no established evidence of optimal global exploration and the fastest convergence resolution, especially with PL in 5 G CPS. Although most of the NIA offers good computation methods, the generic GSA still suffers from premature convergence, poor local search ability, and a lack of effective acceleration mechanisms. It is equally clear that PL is a key factor that gives an idea of the network coverage for CP application provisioning. Hence, the design of a reliable CP wireless system demands precise PL prediction models. The works failed to highlight that future CP networks will depend on extra super high frequency and mm-wave spectrum frequency because of scalable and massive bandwidth demand. However, most PL studies on 5 G lack detailed modelling of CP sensitivity based on GSA. Also, the propagation models often fail to highlight new empirical improvements needed for characterising communication channels in both indoor and outdoor environments for SHF and mm-wave services. In Section 3, various empirical models are modified for PL stability and sensitivity, especially for CP applications.

3. Empirical propagation models

This section discusses the empirical propagation models needed for CP service provisioning. These baseline standards are designed for the analysis of CP mobile radio signals in different terrains. The following signal propagation models are investigated for the initial CP model deployment [46].

3.1. CP Okumura-Hata

The Okumura-Hata PL model is an empirical model for modelling urban signal propagation. It applies over a frequency range of 150 MHz to 1500 MHz. The height of the Base Station (BS) antenna (h_{bt}) can vary up to 200 m depending on the terrain characteristics [46,47]. The path loss model (PL_P) is expressed as follows:

$$PL_P \text{ (dB)} = 69.61 + 26.21 * \log_{10} f_c - 13.81 * \log_{10} h_{bt} - y(h_{mts}) + P_{sys} \quad (1)$$

where:

$$P_{sys} = [44.92 - 6.62 * \log_{10}(h_{mt})] * \log_{10}(d)$$

f_c is the transmission frequency (MHz), h_{bt} is the BS antenna height (m), h_{mt} is the MS antenna height (m), $y(h_{mts})$ is the mobile antenna correction factor, d is the distance between the BS and MS (km).

The antenna correction factor $y(h_{mts})$ for large cities is given by:

For $f_c \leq 300$ MHz:

$$y(h_{mts}) = 8.3 * [\log_{10}(1.54 * (h_{mts}))^2 - 1.1 \text{ dB}] \quad (2)$$

For $f_c > 300$ MHz:

$$y(h_{mts}) = 3.2 * [\log_{10}(11.75 * (h_{mts}))^2 - 4.97 \text{ dB}] \quad (3)$$

The antenna correction factor $a(h_{mts})$ for medium-sized cities is expressed as:

$$y(h_{mts}) = 1.1 * [\log_{10}(f_c) - 0.7] * h_{mt} - [1.56 * \log_{10}(f_c) - 0.8] \text{ dB} \quad (4)$$

For suburban areas, the Okumura-Hata PL calculation is given as:

$$PL_P \text{ (dB)} = PL_P \text{ (urban) dB} - 2 * [\log_{10}(f_c/28)]^2 - 5.5$$

This model is valuable for estimating PL in various urban environments, considering antenna heights, frequency, and correction factors for different city sizes.

3.2. CP cost 231- Hata

The Okumura model, which was created initially by a European

cooperative research team, is expanded upon in the COST 231-Hata model. This model runs in the frequency range of 1500–2000 MHz and considers base station (BS) antenna heights of 30–200 m, as well as distances of 1–20 km between the BS and MS antennas [48]. In this model, the PL is written as follows:

$$PL_P \text{ (dB)} = P_0 - 13.81 \log_{10} h_{bt} - y(h_{mts}) + P_1 + C_{ACF} \quad (6)$$

where;

$$P_0 = 46.3 + 33.9 \log_{10} f_c$$

$$P_1 = [44.92 - 6.62 \log_{10} h_{mt}] \log_{10} d$$

C_{ACF} denotes the environmental correction factor, i.e., (0 dB = suburban areas and 3 dB = urban areas). Additionally, the correction factor for the antenna, denoted as $y(h_{mts})$, depends on whether the city is highly populated or small-sized and is defined by eqs. (2) and (3), respectively.

3.3. CP-Ericsson model

The Ericsson 9999 model employs a predictive approach to estimate the Path Loss (PL) by dynamically adjusting network parameters based on the characteristics of the propagation terrain. This model operates within a carrier frequency range of up to 1900 MHz [49]. The PL model is defined in Eq. (7).

$$PL_P \text{ (dB)} = k_0 + k_1 \log(d) + k_2 \log(h_{bt}) + K_j - 3.2 [\log(11.8 h_{mt})^2] + G(f_c) \quad (7)$$

where $G(f_c) = 44.5 \log(f_c) - 4.8 [\log(f_c)]^2$

$$K_j = [k_3 \log(h_{bt}) \log(d)]$$

$g(f_c)$ = frequency correction factor.

Table 2 shows the main terrain correction details for PL.

3.4. CP-Electronic communication Committee- Model

The ECC model extrapolates Okumura measurements, with certain assumptions that were adjusted as detailed in [50]. The PL model is represented by eq. (9).

$$PL_P \text{ (dB)} = A_{FSA} + A_{MPL} - G_{tx} - G_{rx} \quad (8)$$

where,

A_{FSA} denotes free space PL, A_{MPL} = PL median variable, G_{tx} = BS antenna gain, G_{rx} = Mobile Station (MS) antenna gain.

The parameter definitions are summarised in (9), (10), and (11).

$$A_{FSA} = 92.35 + 20 \log(d) + 20 \log(f_c) \quad (9)$$

$$A_{MPL} = 20.4 + 9.8 \log(d) + 7.9 \log(f_c) + 9.6 [\log(f_c)]^2 \quad (10)$$

$$G_{tx} = \log\left(\frac{h_{bt}}{200}\right) [13.9 + 5.8(\log d)^2] \quad (11)$$

Where h_{bt} represents the BS antenna height above the terrain and d is the distance.

For the CAV MS, antenna gain factor in suburban and rural areas, we have:

$$G_{rx} = [42.6 + 13.7 \log(f_c)] [\log(h_{mt}) - 0.59] \quad (12)$$

Table 2

Ericsson model Terrain Parameters.

Deployment Environment	k_0	k_1	k_2	k_3
PL_Urban	37.21	30.19	12.10	0.11
PL_Suburban	43.21	67.92	12.10	0.12
PL_Rural	46.96	100.5	12.10	0.13

Table 3

Summary of Path Loss propagation Models, limitations, and optimisation schemes.

PL Propagation Models	Model Description/Attributes	Considerations	Limitations
Okumura-Hata [46,47]	<ul style="list-style-type: none"> – Empirical model for macrocellular environments and urban areas. – Designed for urban signal propagation (150 MHz to 1500 MHz). – Accounts for Base Station (BS) antenna height variations. – Formula includes PL calculation and correction factors 	<ul style="list-style-type: none"> – First created for conditions that were macrocellular, which limits its applicability to small cells and interior settings for driverless cars. – Inaccurate forecasting of signal behaviour in challenging urban canyons or uneven terrain. – Assumes that the surroundings are littered uniformly. 	<ul style="list-style-type: none"> – does not account for parameter sensitivity – slow convergence – unsuitable for complex real-time problems. – inappropriate for high-dimensional spaces. – does not account for PL repulsion parameters.
COST 231-Hata [48]	<ul style="list-style-type: none"> – Empirical model for cellular network planning, primarily used in certain frequency bands. – An extension of the Okumura model (1500–2000 MHz). – Considers BS antenna heights and distances. – PL calculation incorporates environmental correction and antenna correction factors. 	<ul style="list-style-type: none"> – May not sufficiently account for variations in geography, such as hilly or mountain-based locations. – designed for specific frequency bands and may not be suitable for other bands. – In cities with tall structures and difficult propagation circumstances, precision is limited. 	<ul style="list-style-type: none"> – The effectiveness for long-range and complicated urban situations is limited due to its applicability to a narrow frequency range, flat terrain assumptions, absence of building shadowing consideration, and so on.
Ericsson [49]	<ul style="list-style-type: none"> – Empirical model used in cellular network planning, suitable for specific frequency bands. – Predictive approach for PL estimation. – Adapts network parameters based on terrain characteristics. 	<ul style="list-style-type: none"> – May not be easily adapted for scenarios involving driverless cars because it was developed for specialised cellular network design. – Limited accuracy in settings with shifting vegetation or challenging terrain. – Propagation Condition Fine-tuning. 	<ul style="list-style-type: none"> – Non-simplicity – Convergence issues, – Non-population based. – Lack of simultaneous exploration of multiple solutions.
ECC-33 [50]	An empirical model with application in specific frequency bands.	<ul style="list-style-type: none"> – Its application is limited since it is designed primarily for a limited range of frequencies. – May not capture granularities/fine-grained variations caused by various environmental factors. – Limited ability to account for unusual channel circumstances. 	<ul style="list-style-type: none"> – Lacks global optimisation. – Suitable only for rural and suburban settings, – Applies to a small frequency range, and it doesn't take complicated urban areas into account. – Might not effectively depict optimal PL in crowded urban areas.
Egli [51]	Empirical model used for predicting radio wave propagation in various environments.	<ul style="list-style-type: none"> – Limited coverage for specific environments or terrains. – Inability to account for various obstacle types and reflections in complex urban environments. – Inappropriate for higher frequency bands. 	<ul style="list-style-type: none"> – Unscaled parameter tuning. – Unsuitable for high-dimensional problems.
COST 231 Walfish-Ikegami (COST-WI) [52]	Empirical model designed for cellular network planning, with a specific focus on PL.	<ul style="list-style-type: none"> – Primarily designed for cellular network planning – Inability to account for the dynamics of CAV environments. – Limited accuracy in NLOS scenarios and complex urban environments. – Sensitive to numerous fluctuations in the terrain. 	<ul style="list-style-type: none"> – Uses terrain data updates and advanced raytracing but lacks global convergence.
Ubiquitous Satellite Aided Radio Propagation (USARP) Model [53]	Uses satellite data to predict radio wave propagation, making it suitable for remote areas.	<ul style="list-style-type: none"> – Relying too heavily on satellite data, which could not always deliver real-time information. – Coverage restrictions in remote or poorly satellite-visible places. – Depending on the quality of the satellite data that is available, accuracy may vary. 	<ul style="list-style-type: none"> – Employs real-time data which may not always be available. – Integration and Kalman filtering with unclear computational cost.
Terrain Integrated Rough Earth Model (TIREM) [54]	Numerical model designed for predicting radio wave propagation over long distances.	<ul style="list-style-type: none"> – Has a focus on long-range radio wave propagation prediction. – Might not be appropriate for applications involving short-range CAVs. – Requires in-depth familiarity with the topography and surrounding surroundings. – When the weather is rapidly changing, accuracy might be compromised. 	<ul style="list-style-type: none"> – Suitability for certain frequency bands and overwater propagation, Limited applicability in complex terrains and urban settings. – Requirements for accurate input data may not always be available. – Needs more parameter tuning and adjustments.
Data-driven PL (PL) [55]	Empirical model enhanced by real-world data and machine learning for adaptability.	<ul style="list-style-type: none"> – May not be useful in locations with little data or for situations not covered by the training dataset if there is not enough data available. – Sensitive to long-term changes in the environment. 	<ul style="list-style-type: none"> – Limited generalizability to different situations – Necessity for considerable and accurate data – Potential biases in the training data.
Lee PL [56]	Empirical model suitable for specific frequency bands with adjustable parameters.	<ul style="list-style-type: none"> – May have limited applicability as it is primarily developed for specific frequency bands. – May not consider fine-grained differences in urban or complicated situations. – Choosing the right model parameters and input data might affect accuracy. 	<ul style="list-style-type: none"> – Does not account for sensitivity to repulsion parameters. – Offers parameter optimization with challenges in high-dimensional spaces.
GSA-PL [31]	A heuristic optimization algorithm for PL optimisation was created to address challenging optimisation issues but was inspired by the gravitational laws.	<ul style="list-style-type: none"> – Sensitivity to parameter settings, a lack of complex theoretical framework, potential slow convergence, difficulties in high-dimensional spaces, sensitivity to repulsion parameters, weak adoption, and potential challenges in effectively exploring some search spaces. 	<ul style="list-style-type: none"> – Uses global nature-based optimisation (i.e., exploitation and exploration) but has near-convergence and adaptation issues. – Challenges in high-dimensional spaces. – Sensitivity issues to repulsion parameters.

(continued on next page)

Table 3 (continued)

PL Propagation Models	Model Description/Attributes	Considerations	Limitations
AGSA-PL (proposed)	<ul style="list-style-type: none"> – Ease of implementation. – adaptability to domains. – flexibility for a range of complex problems. – quick convergence to solutions. – population-based exploration – global optimization. capabilities. – intuitive behaviour inspired by gravitation. 	The overall objective of the AGSA optimization technique is to repeatedly update the positions of driverless agents according to gravitational forces, which results in the identification of optimal solutions (i.e., best PL) within the predetermined search space. The limitation is that the optimisation follows a set of established constraints and exit conditions.	No evidence has been established yet.

And for MS gain factor in dense urban areas:

$$G_{rx} = 0.76 (h_{mt}) - 1.86 \quad (13)$$

Where h_{bt} represents the MS antenna height above the terrain.

3.5. CP-Egli propagation model for path loss prediction

The Egli model is a valuable tool for predicting PL in various terrain scenarios. This model excels in scenarios where there are no significant obstructions within the communication channel. It applies to operation frequencies ranging from 45 MHz to 900 MHz, offering reliable predictions for communication distances of up to 50 km [51]. The mathematical formulation of the Egli model is as follows:

$$PL_{Egli}(\text{dB}) = 20\log f_c + P_{sys} + 76.5 - 10\log h_{mt}, \text{ for } h_{mt} \leq 15\text{m} \quad (14)$$

$$PL_{Egli}(\text{dB}) = 20\log f_c + P_{sys} + 86.9 - 10\log h_{mt}, \text{ for } h_{mt} > 15\text{m} \quad (15)$$

where,

$$P_{sys} = 40\log d - 20\log h_{bt}, P_{sys} \text{ is the system factor.}$$

Eqs. (1) to (15) will be used to derive PL comparison later in Section 7.

A summary of several PL Propagation models, their essential characteristics, factors to consider, limitations, and optimization plans for these models is given in Table 3.

In Section 4, this paper introduces CP-AGSA as a novel optimisation approach for addressing PL challenges in CPS, while showcasing the effectiveness of the algorithm through empirical modelling, analysis, and validation against existing models. Its potential applications in improving signal strength prediction for CPS scenarios, particularly in the context of CAVs in 5 G networks will be discussed.

4. Cyber-physical gravitation search algorithm (CP-AGSA)

4.1. Optimisation framework

We now look at an enhanced optimisation technique (i.e., CP-AGSA) proposed to address the PL problem. CP-AGSA facilitates the agile movement of mobile objects (denoted as θ) in the solution space, striking a balance between exploration and exploitation for efficient solution search.

This optimisation method is specifically applied to the CAV optimisation problem, focusing on the gravitational search algorithmic steps (A-G) for a population of space-moving node particles. The proposed scheme exhibits a notably efficient convergence rate compared to conventional PL approaches.

In practical terms, the gravitational pull exerted by other node particles $\prod_{j \neq i}$ induces their migration toward the particle with the highest mass (μ), representing the ideal position to optimise service efficiency. The interplay between exploration (β) and exploitation (γ) is central to heuristic search algorithms. β signifies the algorithm's capacity to thoroughly explore the entire solution space, preventing it from getting trapped in local optima solutions. In contrast, γ represents the algorithm's ability to search a limited area for the best solution (δ). These two aspects, β and γ , are inversely related, with an increase in

exploration leading to a decrease in β .

The dynamic adjustment of γ and β during each algorithm iteration is crucial. In the initial stages, a higher emphasis on exploration is necessary to avoid falling into local optima solutions (φ). Thus, exploration capability should be set to a high value. However, as the algorithm progresses, exploitation capability becomes more critical, aiding the algorithm in swiftly converging toward the optimal solution. This transition optimally balances the trade-off between exploration and exploitation, offering a faster convergence rate and more effective global search. Our CP-GSA is based on the principles of gravity and mass interaction in CP space. Movement in this space is analogous to global movement, wherein heavier masses gravitate toward other objects. The gradual movement of heavier masses in CP space facilitates efficient signal transmission, resembling the exploitation step. The gravitational force (f) between two objects is mathematically expressed as [57]:

$$f = \frac{G(M_a M_b)}{D^2} \quad (16)$$

where G is the constant due to gravity, M_a and M_b are the masses agent, while D is the distance between objects. The implementation steps for CP-GSA are outlined below:

Step A: Initialisation: Data (agent) points are randomly initialised. The i^{th} position of data denoted as U_i is defined as:

$$U_i = (u_i^1, u_i^2, u_i^3, u_i^4, \dots, u_i^y), \text{ for } i = 1, 2, 3, \dots, y \quad (17)$$

where, u_i is the position of i^{th} agent (data points in the channel)

Step B: Fitness Evaluation: Evaluate the fitness of each agent for j^{th} iteration at time t . Define good (t) and poor(t) as follows:

$$\text{good}(t) = \max \{fit_j(t) \mid j \in 1, \dots, Y\} \quad (18)$$

$$\text{poor}(t) = \min \{fit_j(t) \mid j \in 1, \dots, Y\} \quad (19)$$

where, $fit_j(t)$ is the fitness value.

Step C: Gravitational Value: The gravitational value $G_r(t)$ is obtained at iteration t ,

$$G_r(t) = G_{r0} e^{(-at/T)} \quad (20)$$

where, $G_{r0} = 90$, $\alpha = 15$ [58].

G_{r0} and at/T reduces with time to control search accuracy, G_{r0} is the initial gravity value, t is the current iteration, α is the decay rate, and T is the total iterations. The force on the agent i from agent j at time t ,

$$F_{ij}^x(t) = G_r(t) \frac{M_{pi}(t) * M_{aj}(t)}{R_{ij}(t)} \quad (21a)$$

where, F_{ij}^x is the applied force on the agent, $R_{ij}(t)$ is the distance between particle j^{th} to i^{th} .

In this case, it is important to give stochastic characteristics to the algorithm by proposing that the total force that acts on agent i in a dimension d be a random weighted sum of d^{th} components of the forces exerted by other agents,

$$F_i^x(t) = \sum_{j=1, j \neq i}^N rand_j F_{ij}^x(t) \quad (21b)$$

where, $rand_j$ is the random variable in the interval [0,1]

To obtain a good compromise between β and γ which reduces the number of agents with the time lapse in (21a), only a set of agents with better mass can apply forces on the other.

However, this condition is carefully deployed as it may reduce β power and increase γ . To avoid trapping in a local optima state, the algorithm must use the β at the initial stage since it prevents the whole search space from falling into the local optima solution. Hence, β capability should be high. However, toward the end of the algorithm, the γ capability should be high enough to enable the algorithm to converge toward the best solution. By the lapse of iteration, β must fade out, and γ increases. Therefore, by controlling β and γ , only the k_{Best} agents will attract other agents thereby improving the performance of AGSA.

In this instance, k_{Best} is a function of time, with the initial value k_0 at the initial stage and decreasing with time. At the initial stage, all agents will apply the force, and as time goes on, k_{Best} is decreased. In the end, only one agent applies the force to the others. Therefore, (21a) can be rewritten as (21c).

$$F_i^x(t) = \sum_{j \in k_{Best}, j \neq i}^N rand_j F_{ij}^x(t) \quad (21c)$$

where k_{Best} is the set of first K agents with the best fitness value and bigger mass.

Step D: Agent's Masses: Calculate the Gravitational mass, $m_i(t)$, and inertia mass, $M_{ii}(t)$ of agent i at iteration t using (22) and (23).

$$m_i(t) = \frac{fit_i(t) - good(t)}{good(t) - poor(t)} \quad (22)$$

$$M_{ii}(t) = \frac{m_i(t)}{\sum_{j=1}^n m_j(t)} \quad (23)$$

where, $m_j(t)$ is the mass of agent j .

Step E: Agent's Acceleration: Apply Newton's 2nd law to compute the acceleration (a). The resulting applied force (f) is directly proportional to mass (M) and is expressed as (24) and (25).

$$f = kma \quad (24)$$

where constant (k) is equal to 1.

Acceleration of agent in the direction x^{th} , according to the law of motion is expressed as

$$a_i^x(t) = \frac{F_i^x(t)}{M_{ii}(t)} \quad (25)$$

where, $a_i^x(t)$ is the acceleration, and $F_i^x(t)$ the total applied force on the agent i^{th} .

Step F: Agent's Velocity and Position: Update the velocity and position of the agent at the next iteration ($t+1$) using eqs. (26) and (27).

$$vel_i^x(t+1) = rand_i * v_i^x(t) + a_i^x(t) \quad (26)$$

$$x_i^x(t+1) = x_i^x(t) + vel_i^x(t+1) \quad (27)$$

where; $vel_i^x(t)$ and $vel_i^x(t+1)$ are the velocities of i^{th} agents during the iteration t & ($t+1$) respectively, $rand_i$ is a random variable in the interval [0,1], $u_i^x(t)$, and $u_i^x(t+1)$ are the positions of i^{th} agents during iteration t and ($t+1$).

Step G: Repeat Steps B to F: Iteratively repeat Steps B to F, allowing each agent to update its position to reach the maximum limit and meet the end criterion. The computational framework for the AGSA algorithm in CAV scenarios is illustrated in Fig. 1. AGSA relies on two key parameters to control the search process: the number of applied agents (k_{Best}) and the gravity constant (G). Initially, k_{Best} explores β , and as the algorithm progresses, G is reduced to enhance the γ capabilities of the algorithm. This approach aligns with the principles of strengthening CAV exploration during the early stages and intensifying exploitation in the later stages. The dynamic adjustment of k_{Best} affects the number of considered CAV objects on the road. This ultimately leads to better trade-offs and ensures high stability in both time and frequency domains, similar to frequency responses discussed in Jing et al. [53].

4.2. CP GSA node-link formulation

This subsection considered the CAV as a CPS control problem whose formulation is resolved with AGSA. It solves the problem of link predictive control (LPC) for PL in both the time and frequency domains. In this case, the input-to-state traffic parameters are introduced while the

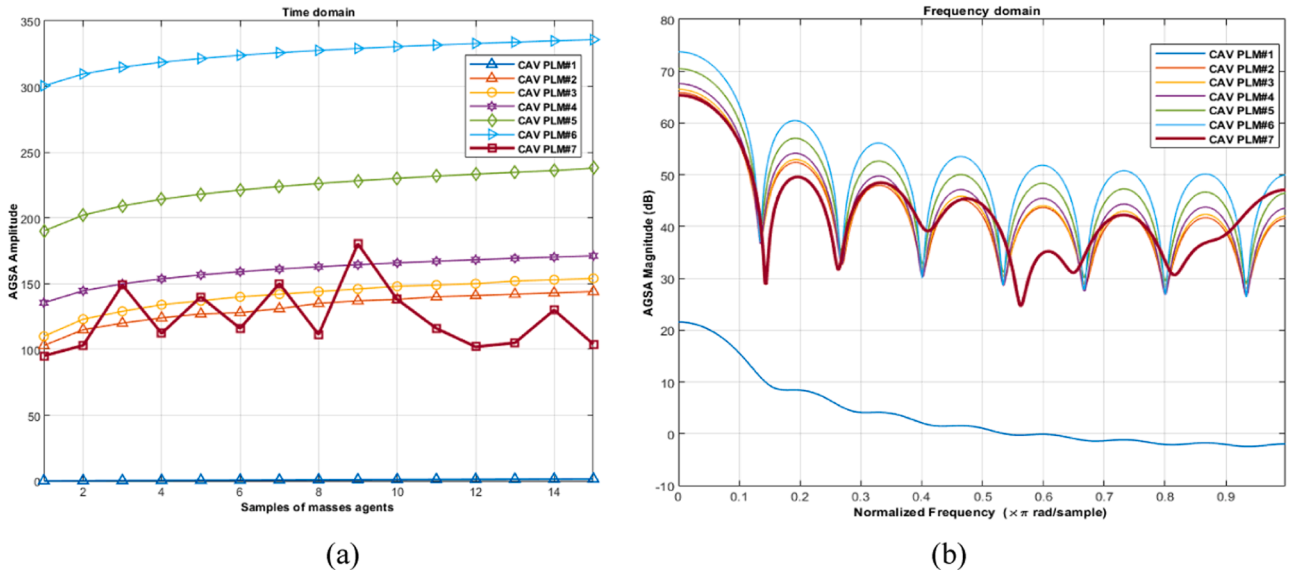


Fig. 1. Influence of AGSA on CAV PL: (a)Time domain (b) Frequency domain with Leakage factor (7.68%), Relative sidelobe attenuation (−15.8 dB), and main width (−3 dB): 0.11719.

Algorithm 1

Optimal Agile PL Label Algorithm (OAPLA).

```

1: Inputs:      PL_Control-CallSchedule  $\{X_{e'v} + X_{e'v'}\}$ ,  $e, N_d, A_v$ 
                History of CAV RAN resources, PL optimisation
Output:      CAV_AGSA
Parameters:  CAV_weight  $\leftarrow$  Empty; // CPS Weighted Moving Average
                PL  $\leftarrow$  0; PLMoving  $\leftarrow$  0; totalPLt  $\leftarrow$  0;
                CPS_PLContainerhistoryItem  $\leftarrow$  null; // PL Pattern

int i  $\leftarrow$  0;
Procedure
Begin ()
    OAPLA ( $S_v; X_{v,v'}$ )
    While  $i < \text{CAV\_edge\_monitorCallSchedule}$  d do
        PLhistoryItem  $\leftarrow$  PLHistoryList.get (PLHistoryList.Size() – CPS_monitorCallSchedule –  $i$ )
        CPS_weight  $\leftarrow$  G;
        CPS_PLMoving  $\leftarrow$  CPS_PLweightedMoving+ (DemandcontainerItem * G);
        total CPS_PL  $\leftarrow$  total CPS_PL+ CPSPL;
         $i++$ ;
    end while
    CAV_DES  $\leftarrow$  CPSweightedMoving / totalCPSWeight;
Return CAV.DES

```

search control strategy is used to demonstrate the effectiveness of the scheme. Now, applying the CAV_node-link design to the issues underlying [Algorithm 1](#) will ensure the effective use of available paths in CP-AGSA as already established in [Section 4](#). This article provides a

formulation for the problem below. Assume a non-zero demand between CAV-ordered pair CP edge nodes. Now, CP-SA node-link formulations.

LP: CP-GSA NLF

CP-GSA 5G Paths Translations - First Step

Algorithm 2

PL Agile Auto-Scaling Non-Saturation Algorithm.

```

// Analyzer
for  $(v, \omega) \in (V \setminus \{S\}) * (V \setminus \{S\})$  do  $f(v, \omega) \leftarrow 0$ ;  $r_f(v, \omega) \leftarrow c(v, \omega)$  od;
 $d(s) \leftarrow |V|$ ;  $Q \leftarrow \emptyset$ ;
for  $v \in V \setminus \{S\}$  do
     $f(s, v) \leftarrow c(s, v)$ ;  $r_f(s, v) \leftarrow 0$ ;
     $f(s, v) \leftarrow c(s, v)$ ;  $r_f(s, v) \leftarrow c(v, s) + c(v, s)$ ;
     $d(v) \leftarrow 0$ ;  $e(v) \leftarrow c(s, v)$ ;
Compute the first CAV_edge in  $A_v$  /*the latest CAV_edge*/;
if  $e(v) > 0$  and  $v \neq t$  then inserts  $v$  into  $Q$  with priority  $d(v)$  f1;
    od
While  $Q \neq \emptyset$  do
    Expunge a vertex  $v$  of the Most significant priority  $d(v)$  within  $Q$ ;  $rel \leftarrow \text{Invalid}$ ;
Recycle
    let  $v, \omega$  be the current edge in  $A_v$ 
    if  $r_f(v, \omega) > 0$  &&  $(v) = d(\omega) + 1$ 
    PUSH ( $N, f, v, \omega; f$ );
        if  $\omega \notin Q$  and  $\omega \neq S, t$  then insert  $\omega$  into  $Q$ 
        With priority  $d(\omega)$  f1
    f1
        if  $e(v) > 0$  then
            if  $vw$  is not the last edge in  $A_v$ 
            then select next CAV_edge in  $A_v$  as CAV_edge.
    Else Relabel ( $N, f, v, d$ );  $rel \leftarrow \text{true}$ ;
    f1
f1
Compute the initial CAV_edge in  $A_v$  as CAV_edge;
Until  $e(v) = 0$  or  $rel = \text{true}$ ;
end if
end return

```

Indices: $d = 1, 2, \dots, D$ CAV_CPS traffic demands $e = 1, 2, \dots, E$ CAV_CPS directed arcs links $v, v' = 1, 2, \dots, V$ CAV_CPS edge nodes**Constants** $a_{ev} = 1$ if arc e originates at node v ; 0, otherwise $b_{ev} = 1$ if arc e terminates in node v ; 0, otherwise C_e Capacity of link e **Variables** $X_{v, v'}$ = total CP traffic assigned to demand originating at node v and terminating in node v' $S_v = \sum_v X_{v, v'}$ total traffic demand clustering at node v X_{ev} continuous non – negative traffic flow selecting all traffic demand coming at node v on arc e **Algorithm 3**

5 G Resource Allocation Scheme + PL Function.

```

// Initiate 5G Call_Resources
for network parameters define ();
    PL_path_loss: calculate PL (dB).
def (network slicing  $\leftarrow$  CAV_edge).
Num_CAV ()
Num_resource_blocks ()
# Generate random CAV data rates and quality of service requirements
CAV_data_rates = random.rand int (num_CAV) # Sub-6Hz
CAV_QoS_requirements = random.randint(num_CAV) # QoS levels (1-10)
    Sort CAV based on their QoS requirements (lower QoS value is better)
    Sort CAV = argsort(num_CAV_QoS_requirements)
# Initialize resource allocation matrix
break:
for CAV in sorted location (L1: L2: L3):
    for  $v \in V\{s\}$  do
         $f(v)$ : resource_allocation  $\leftarrow$  zeros ((CAV_users, num_resource_blocks))
        # FCFS resource allocation
def calculate_PL (distance, frequency, tx_height, rx_height, shadow_fading_stddev=4.0):
    calculate_PL  $\leftarrow$  Parameters ()
    distance: Distance between the transmitter and receiver (in meters).
    frequency: Transmission frequency (in Hertz).
    x-height: Height of the transmitter antenna (in meters).
    rx_height: Height of the receiver antenna (in meters).
    shadow_fading_stddev: Standard deviation (default: ( ) dB).
    break:
    path_loss: Calculated path loss in dB.
break:
Compute the first CAV_edge in  $A_v$  /*the latest CAV_edge*/;

While  $\beta(\mu) \neq \vartheta$  do
    forward error correction (FEC) ()
    automatic repeat request (ARQ) ()
    expunge a vertex  $v$  of the most significant PL deviation  $d(PL)$  within  $f(v)$ ; PL  $\leftarrow$  Invalid;
    requested_blocks  $\leftarrow$  CAV_data_rates[+1]
    allocated_blocks  $\leftarrow$  min (requested_blocks, num_resource_blocks)
    # Allocate the requested number of blocks
    resource_allocation [CAV: allocated_blocks] = 1
    CAV_resource_blocks  $\leftarrow$  CPU: Memory allocated blocks.
    break:
if ( $v$ ) is not the last edge in  $A_v$ 
    then select next CAV_edge in  $A_v$  as CAV.
    break:
Recycle
Until  $\beta(\mu) = 0$ ;
break:
end break:

```

Objective

$$\text{Max } t \quad (28a)$$

Constraints

$$\sum_e b_{e,v'} X_{ev} - \sum_e a_{e,v'} X_{ev} = X_{v,v'}, \quad v, v' = 1, 2, \dots, V \quad v \neq v' \quad (28b)$$

$$S_v = \sum_v X_{v,v'} \quad v = 1, 2, \dots, V \quad (28c)$$

$$\sum_e a_{e,v} X_{ev} = S_v \quad v = 1, 2, \dots, V \quad (28d)$$

$$t - X_{v,v'} \leq 0 \quad v, v' = 1, 2, \dots, V \quad v \neq v' \quad (28e)$$

$$\sum_v X_{ev} \leq C_e \quad e = 1, 2, \dots, E. \quad (28f)$$

In this formulation, constraint (28d) requires that the entire demand traffic S_v produced in node v navigate out of node v . The constraint (28b) supports that the component of the flow $X_{v,v'}$ that originated at node v . It is intended for node v' to remain in v' .

Keep in mind that $X_{v,v'}$ is the same as X_d in the formulation. To use the CPS_node-link formulation in CAV-CPS, directed graphs must have directed linkages. Therefore, if the links in the legacy network are undirected, (i.e., two oppositely directed arcs are attached with each link e (e' and e' between its end nodes), we then replace constraint (28f) with (28g).

$$\sum_v (X_{ev} + X_{ev'}) \leq C_e \quad e = 1, 2, \dots, E. \quad (28g)$$

Algorithm 2 shows the pre-flow service provision Algorithm. The idea is to constantly update the lookup tables of AGSA at CAV_edge (connected vehicles). Assume that the flow network, $N_d = (G, c, s, t)$ contains a symmetric digraph G that is determined by incidence lists A_v . Furthermore, by making the *rel* a Boolean variable, let Q denote a CP-GSA path loss priority queue with the PL priority function d . The PL Agile auto-scaling non-saturation algorithm reduces latency (execution time), channel error, and network size.

4.3. Implemented 5G network algorithm

In implementing the 5 G CAV network algorithm, the testbed handles wireless communication/networking protocols and signal processing. On top of legacy device algorithms, this paper used CAV resource allocation with Hybrid Automatic Repeat reQuest (HARQ) to improve data transmission reliability. HARQ is enabled in 5 G CAV to enhance the reliability of data transmission. CAV-HARQ integrates forward error correction (FEC) and automatic repeat request (ARQ) end-to-end while synergistically improving the efficiency of recovering lost or corrupted data. Network slicing is another scheme used to divide a single CAV physical network into multiple virtual networks while supporting various radio access networks (RANs), and its services. For example, consider CAV communication. The vehicle requires low latency but not necessarily high throughput. On the other hand, a streaming service

Table 4
5 G Drive Test Parameters.

CAV_Carrier Frequency	3.5 GHz
Tx Power	46 dBm
Tx height	45 m
Tx Gain	2.0 dBi
Rx Gain	1.8 dBi
Mobile station height	1.6 m
Radiating power (EIRP)	55dbm
Interference Margin (I)	3.0

Table 5

CAV drive Test locations.

(Locations)	Area in Wales
L1	Tesco- Pontypridd Park
L2	Wood Road
L3	Graig Street

Table 6

Measurement Study at Pontypridd Terrain.

Dist. (km)	Measured $PL_P(d_0)$ (dB) L 1	Measured $PL_P(d_0)$ (dB) L 2	Measured $PL_P(d_0)$ dB L 3	Average Measured $L_{PM}(d_0)$ dB
0.1	95.1	87.20	100.10	94.13
0.2	103.1	124.00	102.00	109.70
0.3	149.0	116.10	118.10	127.73
0.4	112.2	102.20	168.30	127.57
0.5	140.0	152.00	112.20	134.73
0.6	116.0	120.30	141.20	125.83
0.7	150.1	104.10	114.10	122.77
0.8	111.3	131.10	134.10	125.50
0.9	180.2	107.20	150.30	145.90
1.0	138.1	119.30	123.10	126.83
1.1	116.0	105.10	135.10	118.73
1.2	102.0	128.20	101.30	110.50
1.3	145.0	116.00	142.10	134.37
1.4	130.0	130.30	110.20	123.50
1.5	104.0	122.10	121.10	115.40

Table 7

CP Regression Analysis for L1 with Measured Data.

Dist. (m)	Measured PL $PL_{PM}(d_0)$ dB	Predicted PL $PL_{PR}(d_i)$ dB	$PL_{PM}(d_0) -$ $PL_{PR}(d_i)$
100	95.1	95.1	0
200	103.1	$95.1 + 3.01 x$	$008 - 3.01 x$
300	149.0	$95.1 + 4.77 x$	$053.9 - 4.77 x$
400	112.2	$95.1 + 6.02 x$	$017.1 - 6.02 x$
500	140.0	$95.1 + 6.99 x$	$044.9 - 6.99 x$
600	116.0	$95.1 + 7.78 x$	$020.9 - 7.78 x$
700	150.1	$95.1 + 8.45 x$	$0055 - 8.45 x$
800	111.3	$95.1 + 9.03 x$	$016.2 - 9.03 x$
900	180.2	$95.1 + 9.54 x$	$085.2 - 9.54 x$
1000	138.1	$95.1 + 10.00 x$	$042.9 - 10.0 x$
1100	116.0	$95.1 + 10.41 x$	$020.9 - 10.41 x$
1200	102.0	$95.1 + 10.79 x$	$006.9 - 10.79 x$
1300	145.0	$95.1 + 11.14 x$	$049.9 - 11.14 x$
1400	130.0	$95.1 + 11.46 x$	$034.9 - 11.46 x$
1500	104.0	$95.1 + 11.76 x$	$08.9 - 11.76 x$

used while driving demands a lot of capacity and needs to minimise the delay. To efficiently utilise the physical network, both services are offered over the same shared physical network using virtual network slices. Network slicing optimises network resources and improves overall performance. **Algorithm 3** describes the above 5 G algorithm where the 5 G parameters are defined while calling the RAN network slicer. Once the rates are verified, the PL loss function isolates distance, frequency, transmitter height, receiver height, and an optional shadow fading standard deviation as inputs. It calculates the PL using the free space PL formula and additional terms for height difference and shadow fading. More advanced PL models, environmental effects, multipath propagation, and other real-world complexities are not considered.

5. USE case scenario

This section adopted the highly provisioned drive Test (HPDT) method for data collection from the Sub-6 GHz network at the Tesco Pontypridd Warehouse study area in Wales. The cell sites in Pontypridd City and its surrounding rural areas are larger than mmWave and

Table 8

Measured, Predicted, Modified, and Enhanced CP-AGSA PL values for L1.

Dist. (km)	OHM (dB)	COST 231 (dB)	Ericc (dB)	Eggl (dB)	ECC-33 (dB)	Measured PL (dB)	Modified (L1) (dB)	Enhanced (AGSA) dB
0.1	100.3	102.8	135.5	190.1	300.5	95.1	109.3	109.0
0.2	110.8	116.2	144.6	202.1	309.5	103.1	113.9	113.6
0.3	116.9	122.4	149.9	209.2	314.7	149.0	117.5	117.2
0.4	121.2	126.7	153.7	214.2	318.4	112.2	120.4	120.2
0.5	124.6	130.1	156.7	218.1	321.3	140.0	123.5	123.2
0.6	127.4	132.8	159.1	221.2	323.7	116.0	126.0	125.1
0.7	129.7	135.2	161.1	223.9	325.7	150.1	128.2	127.8
0.8	131.7	137.2	162.9	226.2	327.4	111.3	130.0	129.7
0.9	133.5	138.9	164.4	228.3	328.9	180.3	131.6	131.3
1.0	135.1	140.5	165.8	230.1	330.3	138.1	133.1	132.8
1.1	136.5	142.0	167.1	231.8	331.5	116.0	134.4	134.1
1.2	137.8	143.3	168.2	233.3	332.7	102.0	135.6	135.3
1.3	139.0	144.5	169.3	234.7	333.7	105.0	136.7	136.4
1.4	140.2	145.6	170.2	236.0	334.7	130.0	137.7	137.4
1.5	141.2	146.7	171.2	237.9	335.6	104.0	138.7	138.4

function at 5 G speeds (i.e., sub-6 GHz standard). Hence, CP-AGSA for an interactive autonomous car used radio link budget parameters obtained from [40] for effective data collection. In this case, the principle of the 5 G radio link budget for the estimation of maximum usable PL between the 5 G NodeB (gNB) and 5 G CAV equipment (CUE) is considered. It illustrates the cell radius both in uplink and downlink locations. In this effort, the signal strength and CP PL were recorded on a log file using TEM 15.0 installed on the Corei3, 2.4 GHz, 8 G laptop. Three Sony-Ericsson Xperia Z3 D6603 devices are used to initiate different network calls with CP software integration. Other equipment interfaced with the laptop are the global positioning system (GPS), and power supply unit. The network parameters employed during the CP driving test are shown in Table 4.

The network has sufficient adaptability and long-range needed for CAV networks. To illustrate the impact of PL on CAVs, this experiment seeks to justify further generalisations on 5 G CAV networks. However, for carrier frequencies: 28 GHz, 39 GHz, 60 GHz, and 72 GHz, PL model equations can be applied for line of sight (LOS) and Non-LOS link budgets.

In this scenario, a low-powered gNB offers indoor coverage of a few tens of meters in crowded metropolitan areas (i.e., Pontypridd City center) to a few hundred meters in more open NLOS conditions, including positions near semi-open market squares. The LOS scenario provides 100Mb/s and 1Gb/s up to around 3.5 km. Now, the recorded data on the log files are later processed with Actix software [59] for further analysis. CPS AGSA optimisation algorithm was then employed to enhance the developed OHM for better performance. The CPS drive test routes and measured data for L1, L2, and L3 are shown in Tables 5 and 6, respectively.

6. Cyber-physical regression analysis

This section introduces Cyber-Physical (CP) regression analysis as a method to analyse the acquired datasets. The PL data obtained from three distinct locations underwent regression analysis. The PL value recorded at 100 m served as the reference measurement, denoted as $PL_{PM}(d_0)$ at distance d_0 . Subsequently, the PL exponent (n) was determined using the quadratic solution technique. Table 7 presents the regression analysis results for distance L1.

In the terrestrial CP radio scenario, the baseline signal strength re-

duces with increasing distance as a result of various channel constraints, including PL, object-obstruction, multipath-fading, and signal-level shadowing effects. The PL ($PL_{(d_i)}$) equation for such terrestrial free space is given as [31]:

$$PL_{(d_i)} = PL_{PM}(d_0) + 10(x) \log \left(\frac{d_i}{d_0} \right) \quad (29)$$

where x represents the PL exponent, d_i gives the distance and d_0 is the distance reference point. To calculate the predicted PL [$PL_P(d_i)$], we incorporate Model Modified Factor (MMF_{sys}) and mobile antenna correction factor an (h_{mts}) into Equ (29) as;

$$PL_P(d_i) \text{ dB} = L_{PM}(d_0) + MMF_{sys} + 10(x) \log \left(\frac{d_i}{d_0} \right) - \text{an} (h_{mts}) \quad (30)$$

where,

$$MMF_{sys} = [26.1 \log_{cf} - 13.8 \log_{ht}]$$

$$\text{an}(h_{mts}) = 3.2 [\log(1.53h_{mt})]^2 - 4.96 \text{ dB}.$$

Considering the distance from 0.1 km to 1.5 km, the model [$PL_{PM}(d_0) - PL_{PR}(d_i)$]² is the summation square error obtained as:

$$1139.919x^2 - 7242.69x + 19,989.57. \quad (31)$$

From (31), the PL exponent (x) is determined using the quadratic solution method $1139.919x^2 - 7242.69x + 19,989.57 = 0$, so that $x = 3.18$. The shadowing error due to channel obstruction resulted in signal deviation. This deviation (δ_{Sdf}) is evaluated using the sum of square errors.

$$\delta_{Sdf} = \frac{1}{N} \left(\sum ([PL_{PM}(d_0) - PL_{PR}(d_i)]^2)^{\frac{1}{2}} \right) \quad (32)$$

Therefore, the shadowing error correction factor, δ_{Sdf} (dB), around a mean value is computed as $\delta_{Sdf} = \frac{1}{15} [(1139.919)(3.2)^2 - 7242.69(3.2) + 19,989.57]^{\frac{1}{2}} = 23.7 \text{ dB}$.

By introducing $PL_{PM}(d_0)_{Ref}$, MMF_{sys} , x and adding δ_{Sdf} (dB) to compensate for terrain error in (30). the modified cyber-physical PL model for L1 is given as:

Table 9

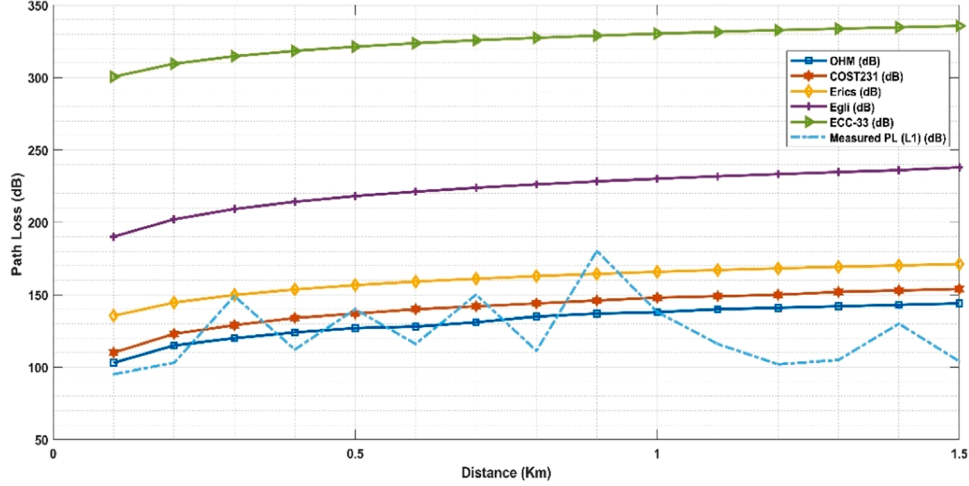
RMSE Analysis of Existing, Modified and Enhanced Models.

Location	Error Metric	OHM (dB)	COST (dB)	Ericsson (dB)	Eggl (dB)	ECC (dB)	Modified Model (dB)	Enhanced AGSA (dB)
L1	RMSE	4.903	10.17	36.49	98.99	201.1	4.290	3.998
L2	RMSE	10.77	16.04	42.36	104.9	206.9	9.875	8.859
L3	MASE	3.497	8.765	35.08	97.58	199.7	2.231	1.870
Average Value	RMSE	6.39	11.66	37.98	100.5	203.6	5.465	4.909

Table 10

MAPE Analysis of Existing, Modified, and Enhanced AGSA models.

Location	Error Metric	OHM (%)	COST (%)	Ericsson (%)	Egli (%)	ECC (%)	Modified Model (%)	Enhanced AGSA
L1	MAPE	0.265	0.549	1.970	5.344	10.86	0.231	0.216
L2	MAPE	0.611	0.909	2.401	5.943	11.73	0.559	0.502
L3	MAPE	0.187	0.468	1.872	5.209	10.66	0.119	0.110
Average Value	MAPE	0.354	0.642	2.081	5.498	11.08	0.303	0.276

**Fig. 2.** Results of PL empirical model and measured data (L1) without AGSA.

$$PL(L1) = 95.1 + [26.1 \log f_c - 13.8 \log h_{bt}] + 10(3.2) \log \left(\frac{d_i}{d_0} \right) - a(h_{mts}) + 23.7 \text{ dB} \quad (33)$$

Substituting the model parameter factors (i.e., $PL_{PM}(d_0)_{Ref}$ - initial measured PL at 100 m away from 5 G base station), PL exponents (x) and shadowing deviation (δ_{SDf}), the modified PL models for L2 and L3 are presented in equ (34) and (35) as:

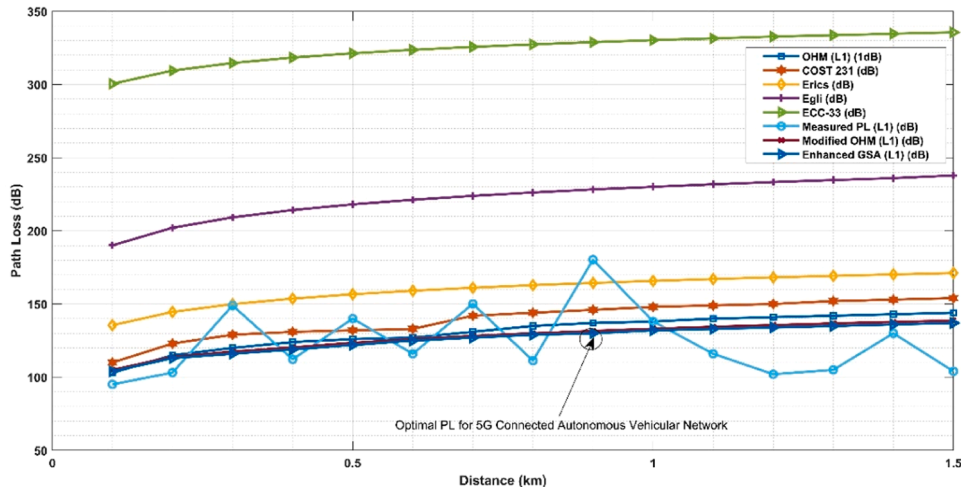
$$PL(L2) = 87.2 + [26.1 \log f_c - 13.8 \log h_{bt}] + 10(3.5) \log \left(\frac{d_i}{d_0} \right) - a(h_{mts}) + 15.4 \text{ dB} \quad (34)$$

$$PL(L3) = 100.1 + [26.1 \log f_c - 13.8 \log h_{bt}] + 10(2.9) \log \left(\frac{d_i}{d_0} \right) - a(h_{mts}) + 19.1 \text{ dB} \quad (35)$$

Therefore, replacing the system baseline parameter factor, the modified PL (i.e., generalised modified) model for the use case is obtained from Equis (33), (34), and (35). Equ. (36) now shows the final use case model.

$$PL(Gen) = 94.1 + [26.1 \log f_c - 13.8 \log h_{bt}] + 10(3.2) \log \left(\frac{d_i}{d_0} \right) - a(h_{mts}) + 19.4 \text{ dB} \quad (36)$$

In this paper, Eq. (36) now represents the modified OHM suitable for

**Fig. 3.** Optimal PL model using empirical and measured datasets for CAV Networks (L1).

deployment in complex CP terrestrial mobile networks. In addition, Table 8 provides CP path loss predicted results in relation to the enhanced CP-AGSA models for L1.

7. Cyber-physical propagation model validation

In this section, we employ two performance metrics, Root Mean Square Error (RMSE) and Mean Absolute Percentage Error (MAPE), to assess the accuracy of both the existing and modified models [31]. The RMSE is represented by Equ (37) as follows:

$$RMSE = \left[\frac{1}{n} \sum_{i=1}^n (PL_{PMi} - PL_{PRi})^2 \right]^{\frac{1}{2}} \quad (37)$$

$$MAPE = \frac{1}{n} \sum_{j=1}^n \left| \frac{PL_{PMi} - PL_{PRi}}{PL_{PMi}} \right| \times 100\% \quad (38)$$

where, $PL_{PMi}(dB)$ represents the measured data, $PL_{PRi}(dB)$ corresponds to the estimated data (i.e., predicted), and "n" stands for summary data point numbers. The RMSE and MAPE result analysis for various models, including the optimised AGSA, are highlighted in Tables 9 and 10.

8. Results discussions

In this section, we present the results of the PL models for CPS service provisioning in the context of 5 G network. We conducted simulations using MATLAB R2018a software and compared the measured data, our modified and enhanced AGSA, as well as existing models. The results are graphically depicted in Figs. 2 through 7, corresponding to different propagation scenarios labelled as L1 to L3.

An illustration of measured PL incidence with existing models is shown in Fig. 2. According to the measured PL scenario, ground reflections are analogous to non-line-of-sight (NLOS) radio propagation, which happens outside the conventional line-of-sight (LOS) between the CAV transmitter and receiver. The innermost Fresnel zone of the park is partially blocked by cars, trees, and other physical objects, therefore the NLOS circumstances appear to be favourable. Specifically, at 0.60 km from the Base Station (BS), we obtained the following PL model values: OHM (127.4 dB), COST (132.8 dB), Erics (159.1 dB), Egli (221.2 dB), and ECC (323.7 dB). Similarly, the model accuracy was computed with MAPE results as follows: 0.265%, 0.549%, 1.970%, 5.344%, and 10.86% respectively. Also, the RMSE was computed to yield OHM (4.903 dB), COST (10.17 dB), Erics (36.49 dB), Egli (98.99 dB), and ECC (201.1 dB) respectively. Notably, the analysis reveals that the ECC-33 model

significantly overestimates the PL due to signal interference and blockage, attributed to the high population density of vehicular users in the 5 G network context.

Fig. 3 illustrates the relationship between PL values and the distance at L1. At 0.60 km from the Base Station (BS), the recorded PL values were as follows: Okumura-Hata (127.4 dB), COST-231 (132.8 dB), Ericsson (159.1 dB), Egli (221.2 dB), ECC-33 (323.7 dB), Modified (126.0 dB), and Enhanced GSA (125.1 dB). Corresponding MAPE values were calculated as Okumura-Hata (0.265%), COST-231 (0.549%), Ericsson (1.970%), Egli (5.344%), ECC-33 (10.86%), Modified (0.231%), and Enhanced GSA (0.216%). Additionally, RMSE results were determined to be Okumura-Hata (4.903 dB), COST-231 (10.17 dB), Ericsson (36.49 dB), Egli (98.99 dB), ECC-33 (201.1 dB), Modified (4.290 dB), and Enhanced GSA (3.998 dB). Notably, the modified model outperformed the existing model in the absence of signal interference. Furthermore, the Enhanced AGSA model exhibited superior performance when compared to all other models. Therefore, it stands as a robust solution to address the challenges associated with inter-symbol interference and signal loss within the 5 G NR network, thereby ensuring seamless connectivity for Connected Autonomous Vehicles (CAVs).

Fig. 4 illustrates a plot of PL responses at Location 2. At 0.60 km from the base Station (BS), the obtained PL values are as follows: 127.4 dB for OHM, 132.8 dB for COST, 159.1 dB for Erics, 221.2 dB for Egli, 323.7 dB for ECC, 126.3 dB for the Modified model, and 125.3 dB for Enhanced GSA. The MAPE results corresponding to these PL values are 0.611%, 0.909%, 2.401%, 5.943%, 11.73%, 0.559%, and 0.502%, respectively. Additionally, the RMSE values for the same set of PL values are 10.77 dB, 16.04 dB, 42.36 dB, 104.90 dB, 206.90 dB, 9.875 dB, and 8.859 dB. These results highlight significant insights for CAVs. ECC-33 appears to have overestimated the PL due to the high traffic density and signal attenuation caused by available shops and tall structures in the terrain. On the other hand, the modified model demonstrates its ability to mitigate network interference and improve signal coverage. Notably, the enhanced AGSA outperforms existing models, offering the lowest PL values in this case study, thereby justifying the convergence expectation for CAVs.

Fig. 5 illustrates the PL observations at location L3. At 0.6 km from the Base Station (BS), the PL responses for different models are as follows: OHM (127.4 dB), COST (132.8 dB), Erics (159.1 dB), Egli (221.2 dB), ECC (323.7 dB), Modified GSA (125.4 dB), and Enhanced GSA (124.0 dB). In terms of MAPE results obtained, the values are 0.187%, 0.468%, 1.872%, 5.209%, 10.66%, 0.119%, and 0.010% for OHM, COST, Erics, Egli, ECC, Modified GSA, and Enhanced GSA, respectively.

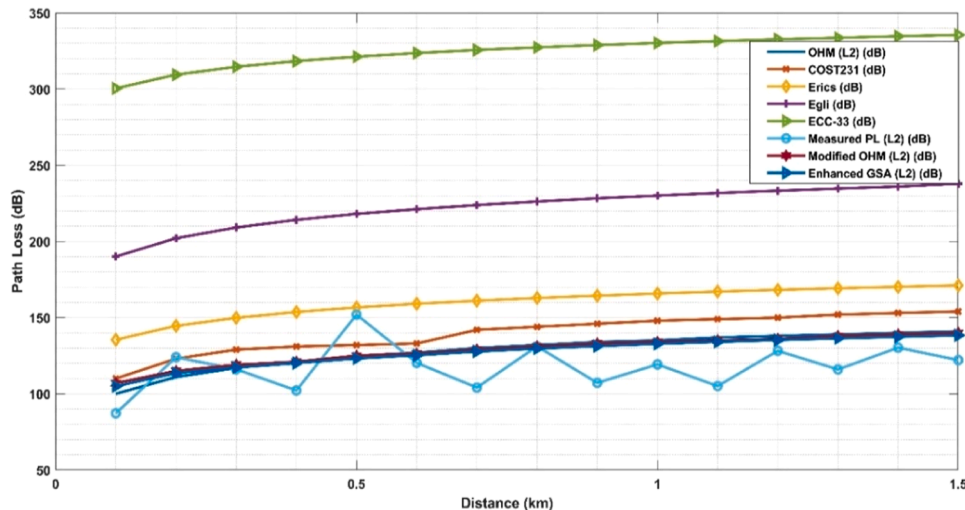


Fig. 4. Optimal PL model using empirical and measured datasets for CAV Networks (L2).

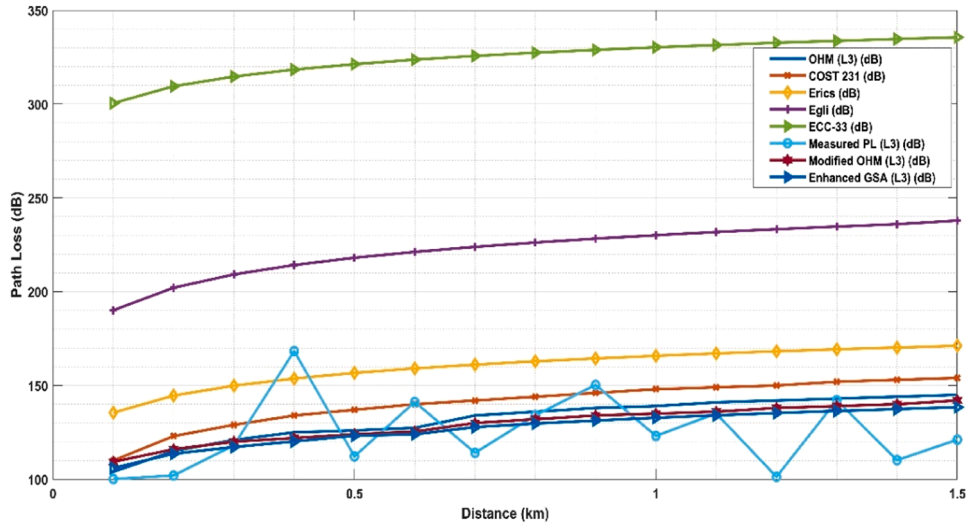


Fig. 5. Optimal PL model using empirical and measured datasets for CAV Networks (L2).

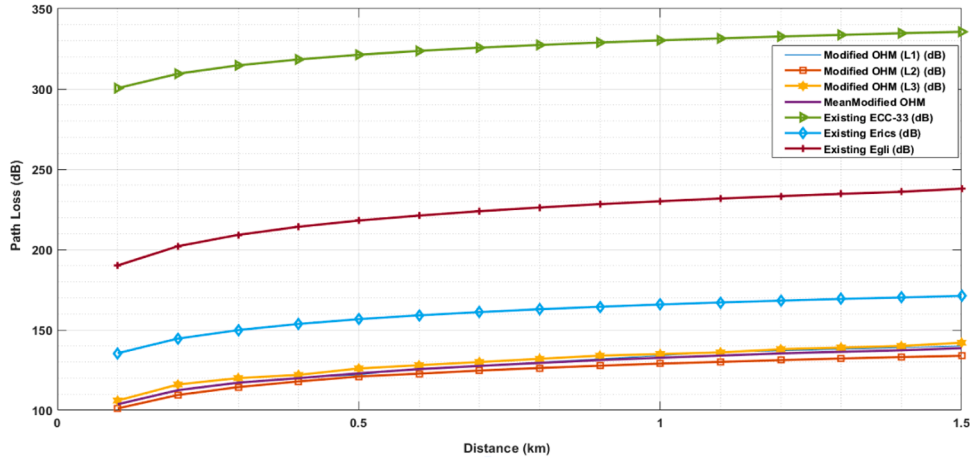


Fig. 6. Optimal PL model using empirical datasets for CAV Networks (L1, L2, and L3).

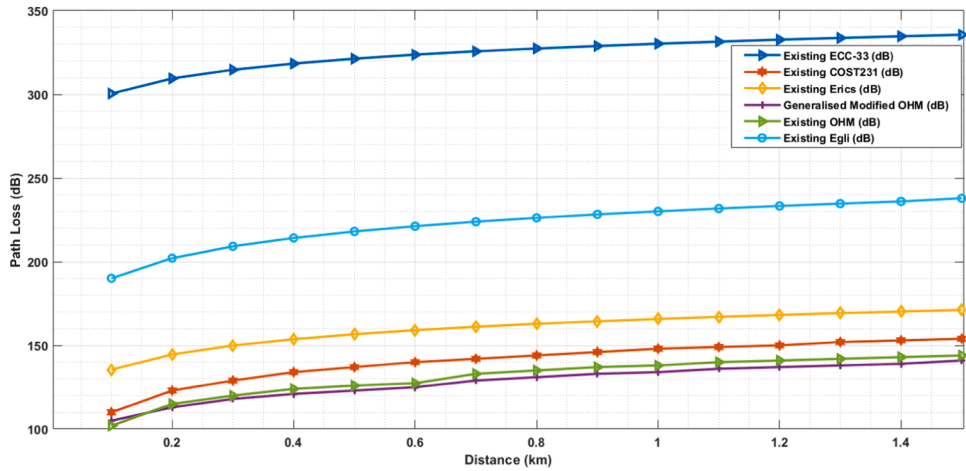


Fig. 7. Generalised OHM PL Performance against distance (L3).

Corresponding Root Mean Square Error (RMSE) results are 3.488 dB, 8.675 dB, 34.99 dB, 98.58 dB, 198.80 dB, 2.322 dB, and 1.881 dB. Remarkably, the improved AGSA outperforms all other models in this scenario. It's worth noting that there was no network interference,

which contributed to efficient service delivery. Consequently, this model exhibits promise for estimating and deploying 5 G NR networks in high-density terrains for CAVs.

Fig. 6 illustrates the PL response at the three different locations,

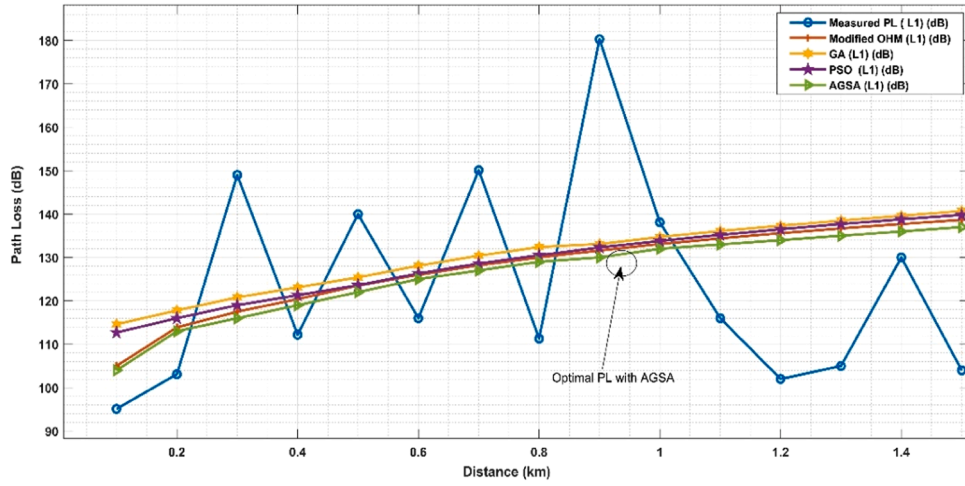


Fig. 8. AGSA Optimised PL deployment against distance (L1).

Table 11
Summary Analysis of Global optimisation schemes.

Location	Error Metric	OHM (%)	GA (%)	PSO (%)	Enhanced AGSA (%)
L1	MAPE	25.55	25.07	24.87	24.51
L2	MAPE	25.22	25.12	24.93	24.73
L3	MAPE	25.24	25.14	25.05	24.57
Average Value	MAPE	59.18	58.57	58.15	57.43

namely L1, L2, and L3. At 0.6 km from the BS, the PL responses are obtained as follows: 324.7 dB for Existing ECC, 159.1 dB for Existing Erics, 221.2 dB for Existing Egli, 128.0 dB for Modified OHM (L3), 122.8 dB for Modified OHM (L2), and 126.0 dB for Modified OHM (L1). Notably, the Mean Modified OHM exhibits superior performance in this measurement environment. Furthermore, it is worth mentioning that no network interference was observed. The model exhibits the potential to alleviate issues such as inter-symbol interference and signal attenuation within the study area. Consequently, it proves to be well-suited for estimating and deploying 5 G NR networks in complex urban terrains like those found in Manchester or Lagos. In this context, it is essential to understand that the PL component represents the reduction in power density experienced by an electromagnetic wave as it propagates

through space. Reducing this path loss can enhance the safety, security, and sustainability of CPS. Moreover, in the context of 5/6 G technologies, an improved path loss algorithm can significantly impact the achievement of three key design objectives. For instance, by reducing its environmental impact in terms of PL, a CAV can become safer. The inherent non-deterministic nature of CAV in an unpredictable physical environment can be addressed with optimal PL schemes.

Fig. 7 depicts the plot of PL values against distance with the Generalised OHM and existing model at L1, L2, and L3. At 0.60 km from BS, the PL responses obtained are 324.7 dB, 221.2 dB, 160.01 dB, 132.8 dB, 127.4 dB, and 124.7 dB, for Existing ECC, Egli, Erics, COST, OHM, and Generalized OHM, respectively. The modified model was observed to perform better than the existing one without symbol interference. The Generalised OHM has the potential to stabilize the effect of inter-symbol interference and signal attenuation in the study area. Hence, the model is reasonable for 5 G CAV deployment in similar terrain. The implication is that PL can be provisioned for service efficiency with modified OHM in context.

9. Global optimisation performance validation

CP-AGSA parameter settings were completed in an experiment with CPU (Intel TM Core i5, 3.8Ghz, 8 G RAM, the following parameters were deployed based on [45], viz: population size, $N = 15$, the minimum

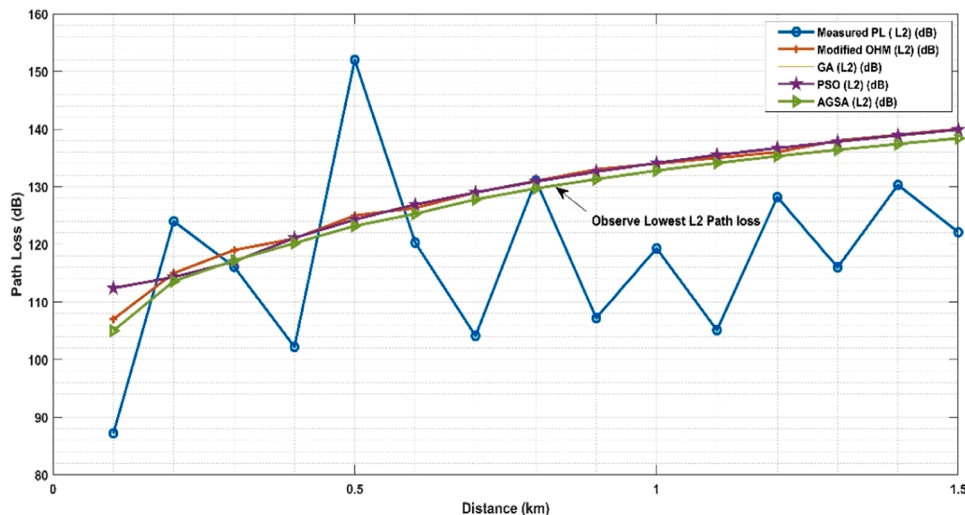


Fig. 9. AGSA Optimised PL deployment against distance (L1).

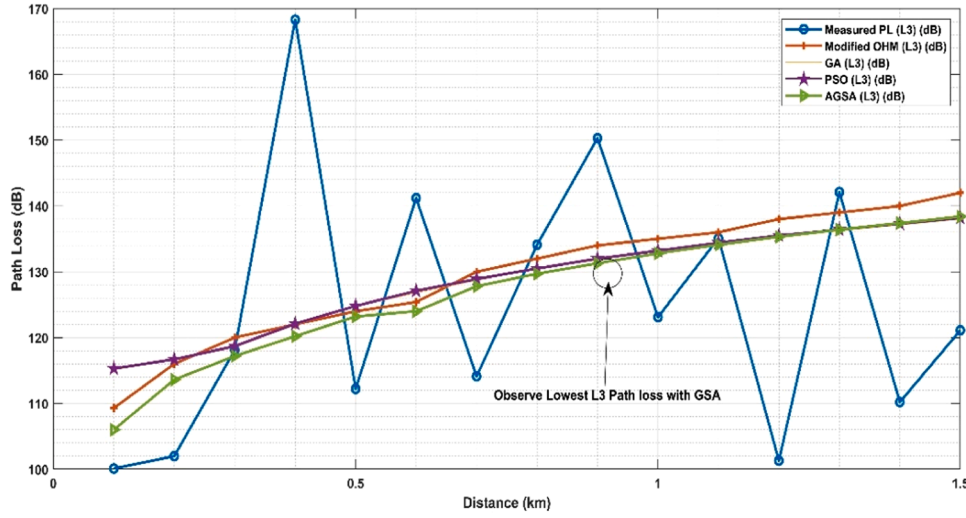


Fig. 10. AGSA Optimised PL deployment against distance (L3).

number of iterations $T = 90$, the gravitational constant, $G_{r0} = 90$, and the decay rate $\alpha = 15$. The global optimisation performance validation was done after the successful completion of the AGSA iterations based on data settings in Section 4. The correspondent data values were obtained per the agent's distance and measured path loss. Afterward, the MATLAB graphics user interface (GUI) was used to obtain the comparative plots of the selected three global algorithms as presented in Figs. 8–10 while table 11 highlighted the findings.

Fig. 8 shows the optimised PL response against distance with measured PL for L1. At 0.70 km from the BS, the PL values are 131.5 dB, 129 dB, 128 dB, and 126 dB for modified OHM, Optimised GA, PSO, and AGSA algorithms, respectively. In this case, the result shows that the optimised AGSA algorithm performs better than all other algorithms. It was observed that there was no network interference leading to efficient service delivery. As such, the algorithm is satisfactory for 5G-CAV deployment in high-density terrains. In this case, real-time safety applications can benefit from AGSA 5 G connected vehicular communication because it offers faster data rates—up to 10 Gbps and significantly reduces latency.

Fig. 9 depicts the optimised result of PL values against distance with measured PL for L2. At 0.70 km from the BS, the PL values obtained are 129.5 dB, 129 dB, 128 dB, and 127 dB for modified OHM, optimised GA, PSO, and AGSA algorithms, respectively. The results show that the AGSA algorithm performed better than GA and PSO algorithms at that terrain. This means that the modified model shows the capacity to mitigate network interference and signal coverage issues when deployed in driverless CPS.

Fig. 10 illustrates a plot showcasing the optimised Path Loss (PL) values in comparison to the measured PL for the L3 scenario. When situated 0.70 km away from the Base Station (BS), the PL values acquired were as follows: 130 dB for the modified OHM model, 129.5 dB for the Optimised Genetic Algorithm (GA), 129 dB for Particle Swarm Optimisation (PSO), and 126.5 dB for Gravitational Search Algorithm (GSA). It is worth noting that the AGSA outperformed both the GA and PSO algorithms in this context. Consequently, the modified model demonstrates promise for accurate estimation and deployment in 5 G NR networks within the studied terrain. This suggests that the utilisation of the modified OHM model can significantly enhance service efficiency.

From Table 11, this work has identified safe applications of the proposed scheme, namely:

- i Full-scale Autonomous Vehicles (AVs) for self-driving operations.

- ii Smart Transportation Systems include traffic management, vehicle-to-infrastructure (V2I), and vehicle-to-vehicle (V2V) communications.
- iii 5 G and beyond for reducing noise interference and optimizing data transmission, benefiting various industries beyond autonomous vehicles.
- iv IoT and Industrial Automation: Noise interference reduction can improve the performance of Industrial Internet of Things (IIoT) applications, such as factory automation, robotics, and critical infrastructure monitoring, where reliable communication is essential.

10. Noise interference wider implications

Driverless cars face signal transmission issues due to noise interference from 4 G, 5 G, and 6 G networks, leading to path loss concerns, especially in edge-driven networks [60]. Results have shown that noise weakens the signal as it propagates, negatively impacting Connected Autonomous Vehicles (CAVs). Noise sources in 4 G/LTE contribute to PL by adding unwanted energy, further deteriorating signal quality during propagation [7,15,40]. To address these noise concerns, an AGSA with error correction coding, adaptive modulation, and interference cancellation could mitigate noise interference and enhance the Signal-to-Noise Ratio (SNR). In 5 G networks, especially at millimetre-wave frequencies, noise interference becomes a significant challenge due to factors like atmospheric absorption and rain attenuation [50]. This paper suggests using AGSA Beamforming, Massive Multiple-Input, Multiple-Output (MIMO), and advanced interference management to combat noise interference in these scenarios, maintaining signal quality, especially in CAVs. Looking ahead to 6 G networks operating in higher frequency bands, potentially reaching terahertz (THz) frequencies, noise interference may arise from various sources like atmospheric gases and electromagnetic interference. This paper recommends advanced AGSA techniques with AI-driven adaptive beamforming, THz band-specific noise filtering, and possibly quantum communication to ensure reliable, high-capacity data transmission. These will address the increasing challenges posed by noise interference in CAVs.

11. Conclusion

This paper introduces the Agile Gravitational Search Algorithm (AGSA) for Connected Autonomous Vehicles (CAV) and assesses its efficiency in optimising path loss in three different locations in Wales, UK. Data was collected over a 5 G network infrastructure for CAVs on the three distinct routes. PL incidences were analysed using CP regression

methods to determine the loss exponent for the terrain. The paper highlights the importance of reducing PL in urban environments where both 5 G New Radio and legacy networks coexist to enhance CAV data processing. amongst the empirical models considered, the Okumura-Hata model was selected and further modified for improved performance. The modified model demonstrated the smallest propagation error compared to other existing empirical models. Evaluation metrics like Root Mean Square Error (RMSE) and Mean Absolute Percentage Error (MAPE) were introduced to assess both existing and enhanced models. Additionally, the paper implemented parameter adjustments for the CP-AGSA algorithm to enhance particle diversity, convergence speed, and accuracy. These adjustments allow the algorithm to escape local optima more efficiently during position updates, ultimately improving convergence performance. The findings indicate that the enhanced AGSA outperforms other nature-inspired algorithms with minimal signal interference. The paper concludes by suggesting future work involving spike neural learning techniques for lightweight path loss optimisation and a deeper investigation into noise interference optimisation.

Declaration of Competing Interest

* None of the authors of this paper has a financial or personal relationship with other people or organizations that could inappropriately influence or bias the content of the paper.

* It is to specifically state that "No Competing interests are at stake and there is No Conflict of Interest" with other people or organizations that could inappropriately influence or bias the content of the paper.

Data availability

Data will be made available on request.

Acknowledgement

This work was supported by the Nigeria Tertiary Education Fund (TETF/ES/UNIV/IMO STATE/TSAS/2021).

References

- [1] Case study- Oxbotica: AI firm develops 'brain' for autonomous vehicles, Available Online: <https://www.gov.uk/government/case-studies/oxbotica-ai-firm-develops-brain-for-autonomous-vehicles>. Retrieved 4th Feb. 2023.
- [2] L. Xu, X. Zhou, Y. Tao, X. Yu, M. Yu, F. Khan, AF relaying secrecy performance prediction for 6G mobile communication networks in industry 5.0, *IEEE Trans. Indus. Info.* 18 (8) (2022) 5485–5493.
- [3] H. Huan, K. Wang, Y. Xie, L. Zhou, Indoor location fingerprinting algorithm based on path loss parameter estimation and Bayesian inference, *IEEE Sens. J.* 23 (3) (2023) 2507–2521.
- [4] R. Liu, A. Liu, Z. Qu and N.N. Xiong, "An UAV-Enabled Intelligent Connected Transportation System With 6G Communications for Internet of Vehicles," in *IEEE Trans on Intelligent Transportation Systems*.
- [5] K. Xu, C.G. Cassandras, W. Xiao, Decentralized time and energy-optimal control of connected and automated vehicles in a roundabout with safety and comfort guarantees, *IEEE Trans. Intell. Transp. Syst.* 24 (1) (2023) 657–672.
- [6] S. Sun, et al., Propagation path loss models for 5G urban micro- and macro-cellular scenarios, in: *Proceedings of the IEEE 83rd Vehicular Technology Conference (VTC Spring)*, Nanjing, China, 2016, pp. 1–6.
- [7] J. Liu, T. Wang, Y. Li, C. Li, Y. Wang, Y. Shen, A transformer-based signal denoising network for AoA estimation in NLoS environments, *IEEE Comm. Lett.* 26 (10) (2022) 2336–2339.
- [8] R. Nebuloni, E. Verdugo, FSO Path Loss Model Based on the Visibility, *IEEE Photonics J.* 14 (2) (2022) 1–9, Art no. 7318609.
- [9] Car and Driver- Autonomous Cars Struggle in Snow, but MIT Has a Solution for That. Published on Feb 25, 2022. Available Online: <https://www.caranddriver.com/news/a31098296/autonomous-cars-snow-mit-researchers-solution/> Retrieved 4th Feb. 2023.
- [10] K.C. Okafor, M.C. Ndinechi, S. Misra, Cyber-physical network architecture for data stream provisioning in complex ecosystems, *Trans. Emerging Tel. Tech.* (2021) e4407, <https://doi.org/10.1002/ett.4407>.
- [11] T.T. Oladimeji, P. Kumar, N.O. Oye, Propagation path loss prediction modelling in enclosed environments for 5G networks: a review, *Heliyon* 13 (8) (2022) e11581, 11.
- [12] H. Mittal, A. Tripathi, A.C. Pandey, et al., Gravitational search algorithm: a comprehensive analysis of recent variants, *Multimed Tools Appl* 80 (2021) 7581–7608.
- [13] B. Raj, I. Ahmady, M.Y.I. Idris, R.M. Noor, A hybrid sperm swarm optimisation and genetic algorithm for unimodal and multimodal optimisation problems, *IEEE Access* 10 (2022) 109580–109596.
- [14] W.J. Shyr, H.C. Juan, C.Y. Tsai, Y.J. Chang, Application of cyber-physical system technology on material color discrimination, *Electronics (Basel)* 11 (2022) 920.
- [15] T. Yang, C. Lv, A secure sensor fusion framework for connected and automated vehicles under sensor attacks, *IEEE Internet Things J.* 9 (22) (2022) 22357–22365.
- [16] P.V. Rajkumar, R. Sandhu, Safety decidability for pre-authorization usage control with identifier attribute domains, *IEEE Trans. Dependable Secure Comput.* 17 (3) (2020) 465–478, 1.
- [17] P.V. Rajkumar, R. Sandhu, Safety decidability for pre-authorization usage control with finite attribute domains, *IEEE Trans. Dependable Secure Comput.* 13 (5) (2016) 582–590.
- [18] P.V. Rajkumar, Soumya K. Ghosh, Dasgupta Pallab, Application specific usage control implementation verification, *Int. J. Network Sec. Appl.* 1 (3) (2009) 116–128.
- [19] N. Jajam, N.P. Challa, K.S.L. Prasanna, C.H.V.S. Deepthi, Arithmetic optimisation with ensemble deep learning SBLSTM-RNN-IGSA model for customer churn prediction, *IEEE Access* 11 (2023) 93111–93128.
- [20] E. Trojovská, M. Dehghani, Clouded leopard optimisation: a new nature-inspired optimisation algorithm, *IEEE Access* 10 (2022) 102876–102906.
- [21] A.R. Nair, S. Kirthiga, Nature inspired approach toward elimination of nonlinearities in SWIPT enabled energy harvesting networks, *IEEE Access* 10 (2022) 100837–100856.
- [22] Y. Yao, H. Liao, X. Li, F. Zhao, X. Yang, S. Hu, Coverage control algorithm for DSNs based on improved gravitational search, *IEEE Sens. J.* 22 (7) (2022) 7340–7351.
- [23] T. Wang, Y. Zhang, N.N. Xiong, S. Wan, S. Shen, S. Huang, An effective edge-intelligent service placement technology for 5G-and-beyond industrial IoT, *IEEE Trans. Indus. Info.* 18 (6) (2022) 4148–4157.
- [24] J. Gazda, E. Ślapanak, G. Bugár, D. Horváth, T. Maksymuk, M. Jo, Unsupervised learning algorithm for intelligent coverage planning and performance optimisation of multitier heterogeneous network, *IEEE Access* 6 (2018) 39807–39819.
- [25] F. Wang, G. Xu, M. Wang, An improved genetic algorithm for constrained optimisation problems, *IEEE Access* 11 (2023) 10032–10044.
- [26] S. Gupta, S. Singh, R. Su, S. Gao, J.C. Bansal, Multiple elite individual guided piecewise search-based differential evolution, *IEEE/CAA J. Automatica Sinica* 10 (1) (2023) 135–158.
- [27] D. Zhu, Z. Huang, L. Xie, C. Zhou, Improved particle swarm based on elastic collision for DNA coding optimisation design, *IEEE Access* 10 (2022) 63592–63605.
- [28] E. Alhenawi, R.A. Khurma, A.A. Sharieh, O. Al-Adwan, A.A. Shorman, F. Shannaq, Parallel ant colony optimisation algorithm for finding the shortest path for mountain climbing, *IEEE Access* 11 (2023) 6185–6196.
- [29] H. Ren, K. Liu, G. Yan, Y. Li, C. Zhan, S. Guo, A Memetic algorithm for cooperative complex task offloading in heterogeneous vehicular networks, *IEEE Trans. Netw. Sci. Eng.* 10 (1) (2023) 189–204.
- [30] S. Lin, F. Li, X. Li, K. Jia, X. Zhang, Improved artificial bee colony algorithm based on multi-strategy synthesis for UAV path planning, *IEEE Access* 10 (2022) 119269–119282.
- [31] R. Jamal, B. Men, N.H. Khan, M.A.Z. Raja, Y. Muhammad, Application of Shannon entropy implementation into a Novel Fractional Particle Swarm Optimisation Gravitational Search Algorithm (FPSOGSA) for optimal reactive power dispatch problem, *IEEE Access* 9 (2021) 2715–2733.
- [32] Ming Ye, R.M. Haralick, L.G. Shapiro, Estimating optical flow using a global matching formulation and graduated optimisation, in: *Proc. Int'l Conf. on Image Processing*, Rochester, NY, USA, 2002.
- [33] Olivas F., Valdez F., Melin P., Sombra A., Castillo O., "Interval type-2 fuzzy logic for dynamic parameter adaptation in a modified gravitational search algorithm. *Inf Sci* 476:159–175.
- [34] A.A. Nagra, F. Han, Q.-H. Ling, S. Mehta, An improved hybrid method combining gravitational search algorithm with dynamic multi swarm particle swarm optimisation, *IEEE Access* 7 (2019) 50388–50399.
- [35] M. Wang, Y. Wan, Z. Ye, X. Gao, X. Lai, A band selection method for airborne hyperspectral image based on chaotic binary coded gravitational search algorithm, *Neurocomputing* 273 (2018) 57–67.
- [36] A. Hossain, N. Ansari, 5G multi-band numerology-based TDD RAN slicing for throughput and latency sensitive services, *IEEE Trans. Mob. Comput.* 22 (3) (2023) 1263–1274, 1.
- [37] S. Mori, K. Mizutani, H. Harada, Software-defined radio-based 5G physical layer experimental platform for highly mobile environments, *IEEE Open J. Vehicular Tech.* 4 (2023) 230–240.
- [38] Z.K. Adeyemo, A.O. Akande, A.O. Fawole, Investigation of some existing prediction models and development of a modified model for UMTS signal in Owerri, Nigeria, *Int. J. Comm. Antenna Propagation* 7 (4) (2017) 290–297.
- [39] A. Sharif, et al., Compact base station antenna based on image theory for UWB/5G RTLS embraced smart parking of driverless cars, *IEEE Access* 7 (2019) 180898–180909.
- [40] Jyrki T.J. Penttinen, 5G network planning and optimization. 5G Explained: Security and Deployment of Advanced Mobile Communications, Wiley, 2019, pp. 255–269, <https://doi.org/10.1002/9781119275695.ch9>.

- [41] B. Lee, D. Ham, J. Choi, S. Kim, K. Yong-Hwa, Genetic algorithm for path loss model selection in signal strength-based indoor localization, *IEEE Sens. J.* 21 (21) (2021) 24285–24296.
- [42] S. Khalid, W.B. Abbas, H.S. Kim, M.T. Niaz, Evolutionary algorithm based capacity maximisation of 5G/B5G hybrid pre-coding systems, *Sensors* 20 (2020) 5338.
- [43] Y. Hervis Santana, R. Martinez Alonso, G. Guillen Nieto, L. Martens, Joseph, D. Plets, Indoor genetic algorithm-based 5G network planning using a machine learning model for path loss estimation, *Appl. Sci.* 12 (2022) 3923.
- [44] Haruna Chiroma, et al., Large scale survey for radio propagation in developing machine learning model for path losses in communication systems, *Sci. Afr.* 19 (2023) e01550, 1–36.
- [45] H. Mittal, A. Tripathi, Avinash C Pandey, R. Pal, Gravitational search algorithm: a comprehensive analysis of recent variants, *Multimedia Tools Appl.* 80 (2021) 7581–7608, 2021.
- [46] A.O. Akande, C.K. Agubor, F.A. Semire, et al., Intelligent empirical model for interference mitigation in 5G mobile network at sub-6GHz transmission frequency, *Int. J. Wireless Inf. Networks* (2023), <https://doi.org/10.1007/s10776-023-00603-z>.
- [47] J. Wang, Y. Li, J. Wang, A low-profile dual-mode slot-patch antenna for 5G millimeter-wave applications, *IEEE Antennas Wirel. Propag. Lett.* 21 (3) (2022) 625–629.
- [48] S.K. Hinga, A.A. Atayero, Deterministic 5G mmwave large-scale 3D path loss model for Lagos Island, Nigeria, *IEEE Access* 9 (2021) 134270–134288.
- [49] S. Sun, et al., Investigation of prediction accuracy, sensitivity, and parameter stability of large-scale propagation path loss models for 5g wireless communications, *IEEE Trans. Veh. Technol.* 65 (5) (2016) 2843–2860.
- [50] E. Abuhdima, et al., Impact of dust and sand on 5G communications for connected vehicles applications, *IEEE J. Radio Frequency Identification* 6 (2022) 229–239.
- [51] R. Dangi, P. Lalwani, G. Choudhary, P. Giovanni, Study and investigation on 5g technology: a systematic review, *Sensors* 22 (26) (2022) 1–32.
- [52] E. Harinda, S. Hosseinzadeh, H. Larijani, R.M. Gibson, Comparative performance analysis of empirical propagation models for lorawan 868MHz in an urban scenario, in: *Proceedings of the IEEE 5th World Forum on Internet of Things (WF-IoT)*, Limerick, Ireland, 2019, pp. 154–159, <https://doi.org/10.1109/WF-IoT.2019.8767245>.
- [53] M. Sousa, P. Vieira, M.P. Queluz, A. Rodrigues, An ubiquitous 2.6GHz radio propagation model for wireless networks using self-supervised learning from satellite images, *IEEE Access* 10 (2022) 78597–78615, <https://doi.org/10.1109/ACCESS.2022.3193486>.
- [54] S. Tadić, M.A. Varner, F. Mitchell, G.D. Durgin, Augmented RF propagation modeling, *IEEE J. Radio Frequency Identification* 7 (2023) 211–221, <https://doi.org/10.1109/JRFID.2023.3285452>.
- [55] A. Bidell, Y. Liu, H. Liang, LoRa gateway placement optimization based on a data-driven low height path loss model, in: *Proceedings of the IEEE Canadian Conference on Electrical and Computer Engineering (CCECE)*, ON, Canada, 2021, pp. 1–6, <https://doi.org/10.1109/CCECE53047.2021.9569055>.
- [56] L.A. Nissirat, M. Ismail, M. Nisirat, M. Singh, Lee's path loss model calibration and prediction for Jiza town, South of Amman city, Jordan at 900 Mhz, in: *Proceedings of the IEEE International RF & Microwave Conference, Seremban, Malaysia*, 2011, pp. 412–415, <https://doi.org/10.1109/RFM.2011.6168779>.
- [57] X. Yu, Q. Zhao, Q. Lin, et al., A grey wolf optimiser-based chaotic gravitational search algorithm for global optimisation, *J. Supercomput.* 79 (2023) 2691–2739.
- [58] Jing Zhao, Haidong Zhu, Yinhua Hu, Enjun Hu, Baole Huang, Tingyu Zhang and Pan Zhang, A gravitational search algorithm based on levy flight, in: *Proc. J. Phys.: Conf. Ser.* 1865 042006, 2021.
- [59] <https://tele-tools.com/actix-analyzer-2020/>.
- [60] K. C. B. Adebisi, Kelvin Anoh, Lightweight multi-hop routing protocol for resource optimisation in edge computing networks, *Internet Things* 22 (2023), <https://doi.org/10.1016/j.iot.2023.100758>.